and IL-6 (*C*) was down-regulated in human CD14+ monocytes treated with tunicamycin, especially at the higher concentration (5 μg/ml). *D–F*, ELISA showed that the production of TNF-α (*D*), IL-1β (*E*), and IL-6 (*F*) in culture media decreased in human monocytes treated with tunicamycin, especially at the higher concentration (5 μg/ml). Data are expressed as means ± SEM of four independent experiments. Open bars, no treatment; shaded bar, treatment with tunicamycin (1 μg/ml); solid bar, treatment with tunicamycin (5 μg/ml). TM, tunicamycin.

Figure 1

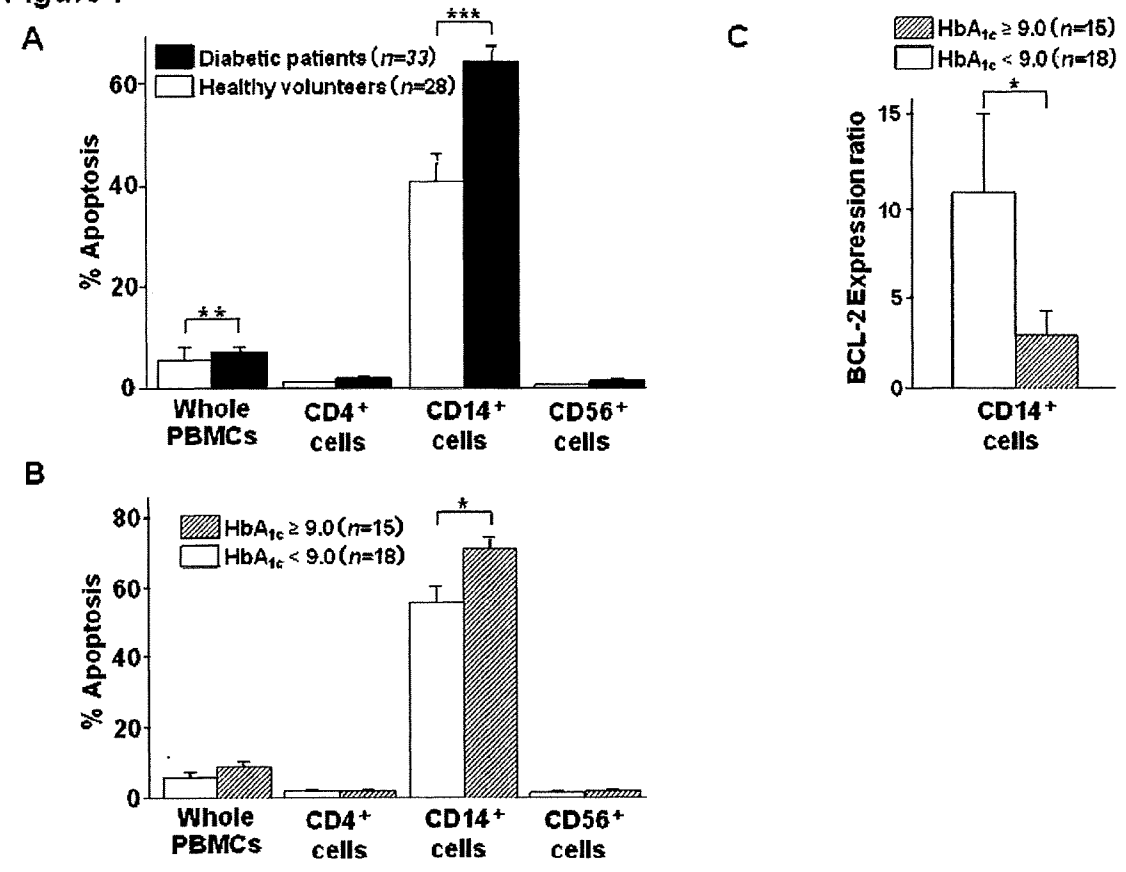

Figure 2

A

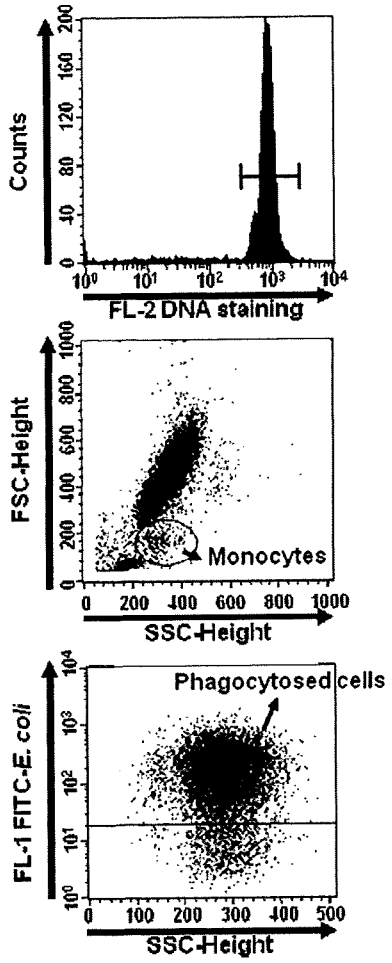
Counts
FL-2 DNA staining
FSC-Height
Monocytes
SSC-Height
FL-1 FITC-E. coli
Phagocytosed cells
SSC-Height

B

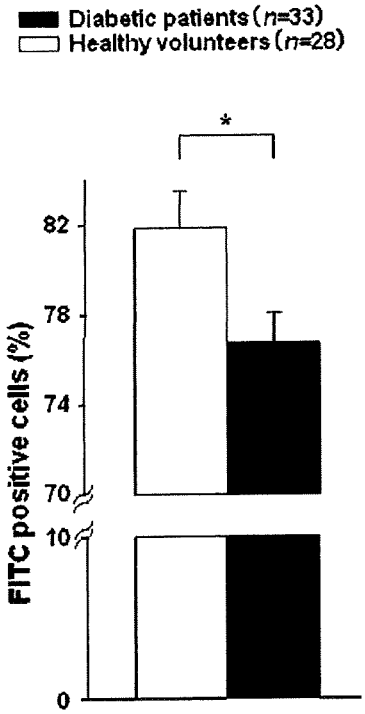
Diabetic patients (n=33)
Healthy volunteers (n=28)
*
FITC positive cells (%)

Figure 3

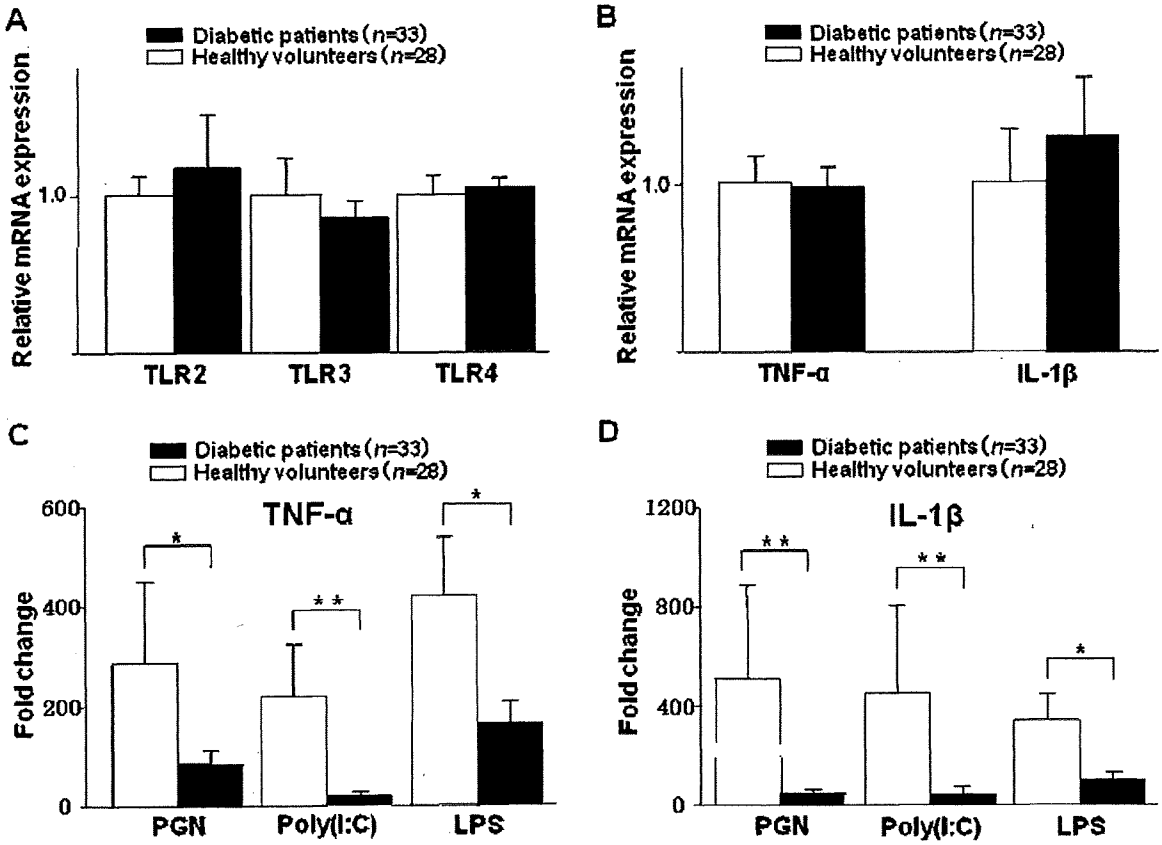
A
Diabetic patients (n=33)
Healthy volunteers (n=28)
Relative mRNA expression
1.0
TLR2
TLR3
TLR4
B
Diabetic patients (n=33)
Healthy volunteers (n=28)
Relative mRNA expression
1.0
TNF-α
IL-1β
C
Diabetic patients (n=33)
Healthy volunteers (n=28)
TNF-α
Fold change
600
400
200
0
*
**
*
PGN
Poly(I:C)
LPS
D
Diabetic patients (n=33)
Healthy volunteers (n=28)
IL-1β
Fold change
1200
800
400
0
**
**
*
PGN
Poly(I:C)
LPS

Figure 4

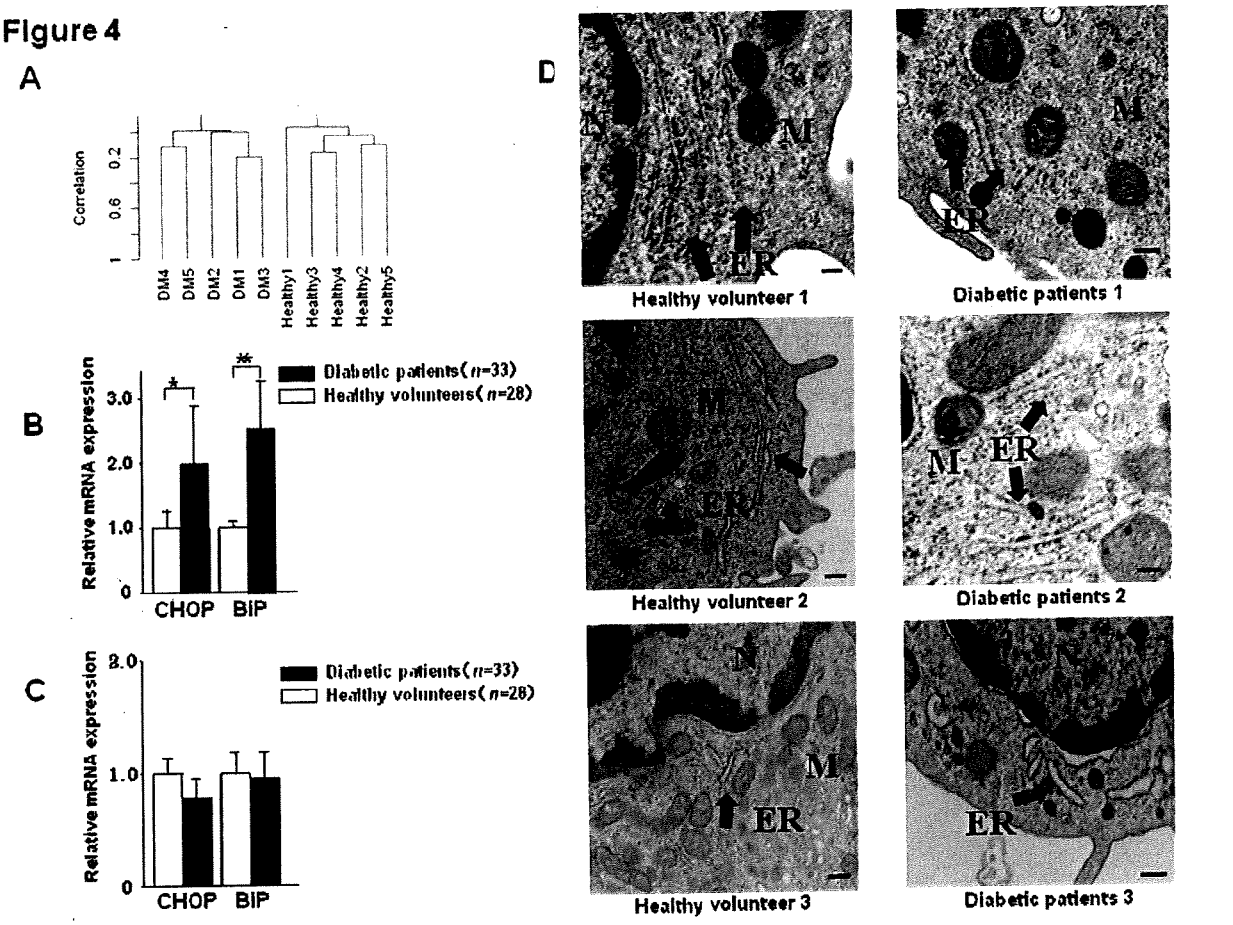
A
Correlation
1
0.6
0.2
DM4
DM5
DM2
DM1
DM3
Healthy1
Healthy3
Healthy4
Healthy2
Healthy5
B
Relative mRNA expression
3.0
2.0
1.0
0
*
*
Diabetic patients(n=33)
Healthy volunteers(n=28)
CHOP
BIP
C
Relative mRNA expression
2.0
1.0
0
Diabetic patients(n=33)
Healthy volunteers(n=28)
CHOP
BIP
D
N
M
ER
Healthy volunteer 1
Diabetic patients 1
Healthy volunteer 2
Diabetic patients 2
Healthy volunteer 3
Diabetic patients 3

Figure 5

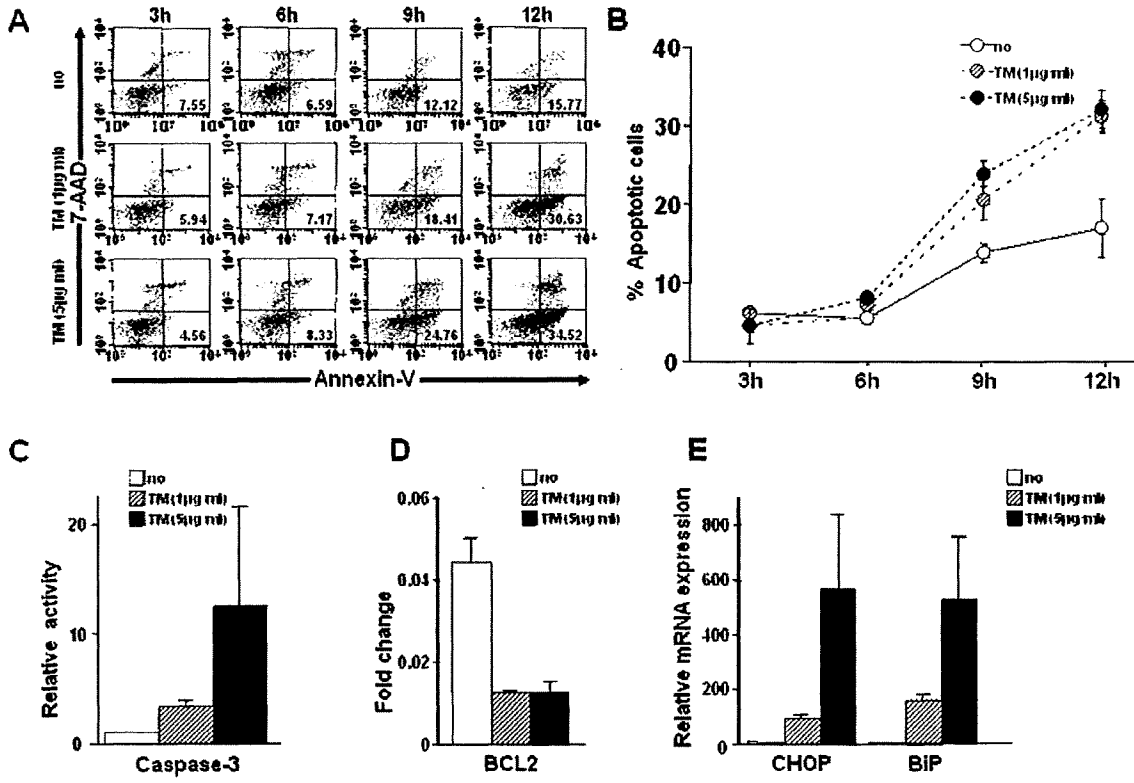
A
3h
6h
9h
12h
no
TM (1μg/ml)
TM (5μg/ml)
7-AAD
Annexin-V
7.55
6.59
12.12
15.77
5.94
7.17
18.41
30.63
4.56
8.33
24.76
34.52
B
% Apoptotic cells
no
TM(1μg/ml)
TM(5μg/ml)
C
Relative activity
Caspase-3
D
Fold change
BCL2
E
Relative mRNA expression
CHOP
BiP

Figure 6

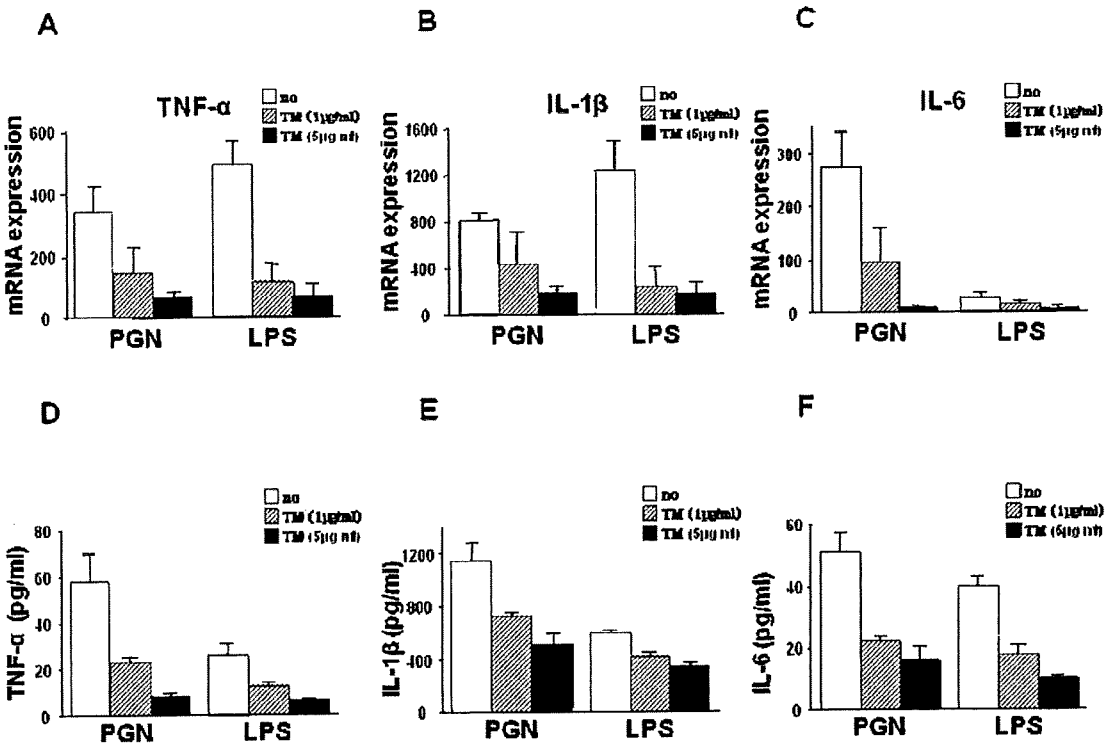
A
TNF-α
mRNA expression
PGN
LPS
B
IL-1β
mRNA expression
PGN
LPS
C
IL-6
mRNA expression
PGN
LPS
D
TNF-α (pg/ml)
PGN
LPS
E
IL-1β (pg/ml)
PGN
LPS
F
IL-6 (pg/ml)
PGN
LPS

Am J Physiol Gastrointest Liver Physiol 296: G850–G859, 2009.
First published January 29, 2009; doi:10.1152/ajpgi.00071.2008.

Signaling pathway via TNF-α/NF-κB in intestinal epithelial cells may be directly involved in colitis-associated carcinogenesis

Michio Onizawa,[1]* Takashi Nagaishi,[1]* Takanori Kanai,[1] Ken-ichi Nagano,[2] Shigeru Oshima,[1] Yasuhiro Nemoto,[1] Atsushi Yoshioka,[1] Teruji Totsuka,[1] Ryuichi Okamoto,[1] Tetsuya Nakamura,[1] Naoya Sakamoto,[1] Kiichiro Tsuchiya,[1] Kazuhiro Aoki,[2] Keiichi Ohya,[2] Hideo Yagita,[3] and Mamoru Watanabe[1]

[1]*Department of Gastroenterology and Hepatology, Graduate School of Medicine and* [2]*Section of Pharmacology, Department of Hard Tissue Engineering, Tokyo Medical and Dental University, Tokyo; and* [3]*Department of Immunology, Juntendo University School of Medicine, Tokyo, Japan*

Submitted 13 February 2008; accepted in final form 11 January 2009

Onizawa M, Nagaishi T, Kanai T, Nagano K, Oshima S, Nemoto Y, Yoshioka A, Totsuka T, Okamoto R, Nakamura T, Sakamoto N, Tsuchiya K, Aoki K, Ohya K, Yagita H, Watanabe M. Signaling pathway via TNF-α/NF-κB in intestinal epithelial cells may be directly involved in colitis-associated carcinogenesis. *Am J Physiol Gastrointest Liver Physiol* 296: G850–G859, 2009. First published January 29, 2009; doi:10.1152/ajpgi.00071.2008.—Treatment with anti-TNF-α MAb has been accepted as a successful maintenance therapy for patients with inflammatory bowel diseases (IBD). Moreover, it has been recently reported that blockade of TNF receptor (TNFR) 1 signaling in infiltrating hematopoietic cells may prevent the development of colitis-associated cancer (CAC). However, it remains unclear whether the TNF-α signaling in epithelial cells is involved in the development of CAC. To investigate this, we studied the effects of anti-TNF-α MAb in an animal model of CAC by administration of azoxymethane (AOM) followed by sequential dextran sodium sulfate (DSS) ingestion. We observed that the NF-κB pathway is activated in colonic epithelia from DSS-administered mice in association with upregulation of TNFR2 rather than TNFR1. Immunoblot analysis also revealed that the TNFR2 upregulation accompanied by the NF-κB activation is further complicated in CAC tissues induced in AOM/DSS-administered mice compared with the nontumor area. Such NF-κB activity in the epithelial cells is significantly suppressed by the treatment of MP6-XT22, an anti-TNF-α MAb. Despite inability to reduce the severity of colitis, sequential administration of MP6-XT22 reduced the numbers and size of tumors in association with the NF-κB inactivation. Taken together, present studies suggest that the TNFR2 signaling in intestinal epithelial cells may be directly involved in the development of CAC with persistent colitis and imply that the maintenance therapy with anti-TNF-α MAb may prevent the development of CAC in patients with long-standing IBD.

tumor necrosis factor-α; colitis-associated cancer; intestinal epithelial cells; carcinogenesis; TNFR2

CROHN'S DISEASE (CD) and ulcerative colitis (UC) are the two major forms of inflammatory bowel diseases (IBD). Although the etiology remains unknown, increasing findings have demonstrated that the involvement of damaged epithelia and activated immune cells in the inflamed mucosa plays an important role in their pathogenesis (15, 23, 46). In addition to the problem of persistent intestinal inflammation in IBD, one of critical complications in patients with long-standing IBD over ~10 years after onset of IBD is colitis-associated cancer (CAC) (9).

It is generally observed that tumors, especially CAC, are usually infiltrated by activated immune cells, such as T cells, neutrophils, macrophages, and dendritic cells, which secrete various cytokines and chemokines (5). Recent works suggest that a major factor in the inflammatory processes involves activated NF-κB pathway (22). Persistent NF-κB activation in the epithelial cells has been suggested to contribute to the development of inflammation-associated cancer including CAC (12). Consistently, it has been demonstrated that activated NF-κB is detected in most tumors (17). Therefore, persistent activation of NF-κB of epithelial cells in response to chronic inflammation may be an important step to intestinal carcinogenesis in CAC in IBD. Consistently, a number of reports have suggested that drugs capable of inhibiting NF-κB activation, such as 5-aminosalicylic acid, reduce the incidence of UC-related colorectal cancer (14). These studies have been approved by the Human Research Committees.

However, it still remains unknown which factors directly induce NF-κB activation in the process of CAC. One possible mediator of NF-κB activation in the epithelial cells of IBD patients is TNF-α, which is markedly elevated in the inflamed intestinal milieu (31). Although TNF-α has been classically considered as an anticancer agent (34), it is currently recognized that chronically elevated TNF-α in tissues may promote cancer growth, invasion, and metastasis (42). Regarding this, animal studies have demonstrated that gene deletion of TNF-α results in the suppression of skin tumor (26). In human studies, anti-TNF-α MAb (infliximab) therapy has been recently proven to be effective in the induction or maintenance of remission in patients with CD (13, 41, 44) or UC (40) refractory to the traditional therapies, such as corticosteroid and/or immunosuppressants.

In this respect, commonly used animal model of IBD-related CAC involves administration of azoxymethane (AOM) followed by repeated dextran sodium sulfate (DSS) ingestion (32). Greten and colleagues (12) demonstrated a decrease in the size of tumors with a decrease in inflammation in the similar AOM/DSS-induced CAC model with myeloid cell-specific deletion of IKK-β, which is an upstream adoptive molecule of NF-κB. Another group had also recently demon-

* M. Onizawa and T. Nagaishi contributed equally to this work.

Address for reprint requests and other correspondence: t. Kanai, Dept. of Gastroenterology and Hepatology, Graduate School, Tokyo Medical and Dental Univ., 1-5-45 Yushima, Bunkyo-ku, Tokyo 113-8519, Japan (e-mail: taka.gast@tmd.ac.jp).

The costs of publication of this article were defrayed in part by the payment of page charges. The article must therefore be hereby marked "*advertisement*" in accordance with 18 U.S.C. Section 1734 solely to indicate this fact.

strated that TNF-α inhibition in the same animal model prevents the development of CAC via blockade of TNF receptor 1 (TNFR1) signaling in infiltrating hematopoietic cells such as neutrophils and macrophages (37). On the other hand, Greten and colleagues also demonstrated that specific deletion of IKK-β in intestinal epithelial cells led to a decrease in the numbers of tumors (initiation) albeit without a decrease in inflammation in the AOM/DSS CAC model. Although the complex background suggests that activation of NF-κB in epithelial cells or hematopoietic cells is involved in the development of CAC, it is still unclear whether TNF-α signaling in the epithelial cells is directly involved in such suppression of carcinogenesis.

In this study, we investigated the NF-κB activity through TNFR1 or 2 signaling specifically in colonic epithelial cells, and assessed the immediate role of anti-TNF-α MAb against epithelial cells in colitis-induced carcinogenesis using the murine AOM/DSS-induced CAC model.

MATERIALS AND METHODS

Animals

Wild-type female C57BL/6 mice (6–8 wk old) were purchased from the Japan Clea (Tokyo, Japan) and were maintained under specific pathogen-free condition. All animal experimentations were performed in accordance with institutional guidelines and were approved by the animal review board of Tokyo Medical and Dental University, Tokyo, Japan.

Cell Culture

Murine colon carcinoma-derived cell line, CT26 (50), were obtained from American Type Culture Collection (Manassas, VA) and maintained in RPMI 1640 (Sigma, St. Louis, MO) supplemented with 10% fetal bovine serum, 500 units/ml penicillin and 100 μg/ml streptomycin (Sigma) at 37°C in 5% CO_2. Cells were seeded at a density of 5×10^5 cells/ml in six-well plates 24 h prior to the experiments with or without recombinant (r) mouse (m) TNF-α (Peprotek, London, UK) with or without blocking anti-TNF-α MAb (MP6-XT22, rat IgG1b), which was obtained from DNAX Research Institute (Palo Alto, CA) and affinity purified (1, 47).

Western Blotting

The stripped colonic epithelial samples from mice were prepared as previously described (16) for assessment of protein and/or mRNA expression. Western blotting was performed as previously described (34). Briefly, 10–100 μg of nucleic extracts or whole protein lysates from either the stripped epithelial samples or CT26 cells were separated by 8–15% SDS-PAGE and each protein expressions were analyzed by use of the following antibodies: anti-mouse TNFR1 polyclonal antibody (PAb), anti-mouse TNFR2 PAb (R&D Systems, Minneapolis, MN), anti-phosphorylated (p)-p65 MAb at serine 536, anti-p65 PAb, anti-p-IκBα MAb at serine 32/36, anti-IκBα PAb, anti-p-Fas-associated death domain (FADD) PAb, anti-cleaved caspase 3 PAb (Cell Signaling Technology, Beverly, MA), anti-FADD PAb (Epitomics, Burlingame, CA), anti-β-actin MAb (Sigma), anti-upstream factor (USF)-2 PAb (Santa Cruz Biotechnology, Santa Cruz, CA), anti-mouse IgG-HRP, anti-rabbit IgG-HRP (GE Healthcare Bio-Sciences, Piscataway, NJ) and anti-goat IgG-HRP (Santa Cruz). Signals were generated with ECL Western Blotting Detection System (GE Healthcare Bio-Sciences).

Real-time PCR. Total cellular RNA was extracted from the stripped epithelial samples described above with RNA-Bee (Tel-Test, Friendswood, TX). Five micrograms of total RNA were used as template for reverse transcription using Superscript Reverse Transcriptase kit (Invitrogen, Carlsbad, CA). The cDNA samples were then applied for PCR with following primer pairs: TNF-α, 5′-CTA CTG GCG CTG CCA AGG CTG T-3′ and 5′-GCC ATG AGG TCC ACC ACC CTG-3′; TNFR1, 5′-GGA AAG TAT GTC CAT TCT AAG AAC AA-3′ and 5′-AGT CAC TCA CCA AGT AGG TTC CTT-3′, TNFR2, 5′-GAG GCC CAA GGG TCT CAG-3′ and 5′-GGC TTC CGT GGG AAG AAT-3′, IL-1β, 5′-TTG ACG GAC CCA AAA GAT-3′ and 5′-GAA GCT GGA TGC TCT CAT CTG-3′, IL-6, 5′-GCT ACC AAA CTG GAT ATA ATC GGA-3′ and 5′-CCA GGT AGC TAT GGT ACT CCA GAA-3′, MIP-2, 5′-AAA ATC ATC CAA AAG ATA CTG AAC AA-3′ and 5′-CTT TGG TTC TTC CGT TGA GG-3′; glyceraldehyde-3-phosphate dehydrogenase (G3PDH), 5′-CTA CTG GCG CTG CCA AGG CAG T-3′ and 5′-GCC ATG AGG TCC ACC ACC CTG-3′ Real time PCR was performed with QuantiTect SYBRgreen PCR kit (Qiagen, Venlo, The Netherlands) using an ABI7500 real-time PCR system and 7500 system SDS software (Applied Biosystems, Foster City, CA). Data of each mRNA expression were shown as the relative amount normalized by that of G3PDH.

Induction of Acute and Chronic Colitis and Colitis-Associated Tumor

Experiment 1. Mice (n = 3–6) intraperitoneally (ip) administered with or without AOM 7 days in advance were treated with 3.0% DSS (molecular weight 10,000; Yokohama Kokusai Bio, Kanagawa, Japan) in drinking water for 5 days (acute phase) followed by treatment with regular water for 2–5 days (recovery phase). Colon samples were then assessed for the histology and expression of TNF-α or TNFR level at recovery phase.

Experiment 2. Mice ip administered with or without AOM 7 days in advance were treated with 3.0% DSS-containing water for 5 days followed by ip injection of control rat IgG (1 mg/mouse) mice (n = 5) or anti-TNF-α MAb (MP6-XT22, 1 mg/mouse) (n = 5) at the end of DSS treatment (*day 5*) before the removal of DSS from drinking water for 2–5 days. Colon samples were then examined for histological changes and cytokine expression profiles. Activities of NF-κB pathway were assessed for the effect of MP6-XT22 in the development of acute colitis.

Experiment 3. To assess the role of TNF-α signaling on the incidence and progression of colon tumors in chronic AOM/DSS-induced CAC model, mice were randomized by body weight into two groups and received AOM ip at *day −7*, followed by three cycles of 3.0% DSS in drinking water for 5 days and regular water for 16 days starting 1 wk after the AOM injection (*day 0*). Mice were treated with 1 mg/mouse of either control IgG or the anti-TNF-α MAb MP6-XT22 weekly starting at the end of the first DSS treatment (*day 5*) (n = 10). Eleven weeks after the first injection of AOM, mice were euthanized and colons were removed, flushed with PBS, fixed as "Swiss rolls" in 10% neutral-buffered formalin at 4°C overnight, and paraffin embedded for histology.

Determination of Clinical Score of Colitis

Body weight, stool consistency, and occult or gross blood per rectum were determined every other day during the colitis induction phase. The colitis clinical score was assessed by trained individuals blinded to the treatment groups (2). The baseline clinical score was determined on *day 0*. Briefly, no weight loss was registered as 0: weight loss of 1–5% from baseline was assigned 1 point; 5–10% was assigned 2 points; 10–20% was assigned 3 points; and >20% was assigned 4 points. For stool consistency, 0 points were assigned for well-formed pellets, 2 points for pasty and semiformed stools that did not adhere to the anus, and 4 points for liquid stools that did adhere to the anus. For rectal bleeding, 0 was assigned for no blood, 2 points for positive Hemoccult, and 4 points for gross bleeding. These scores were added resulting in a total clinical score ranging from 0 (healthy) to 12 (maximal activity of colitis).

Histological Scoring of Colitis and CAC

Tissue samples were fixed in 10% neutral-buffered formalin. For the assessment of colitis, paraffin-embedded sections (5 μm) were stained with hematoxylin and eosin (H&E). The sections were analyzed without prior knowledge of the type of treatments. The degree of inflammation in the colon was graded according to the previously described scoring system (2). Briefly, the presence of occasional inflammatory cells in the lamina propria was assigned a value of 0; increased numbers of inflammatory cells in the lamina propria a value 1, confluence of inflammatory cells, extending into the submucosa a value of 2, and transmural extension of the infiltrate a value of 3. For tissue damage, no mucosal damage was scored as 0; discrete lymphoepithelial lesions were scored as 1; surface mucosal erosion or focal ulceration was scored as 2; and extensive mucosal damage and extension into deeper structures of the bowel wall were scored as 3. The combined histological score ranged from 0 (no changes) to 6 (extensive cell infiltration and tissue damage). For CAC assessment, sections (5 μm) were cut stepwise (200 μm) through the complete block and stained with H&E. Tumor counts were performed in a blinded fashion.

Immunohistochemistry

Colon samples for immunohistochemistry were embedded into OCT compound, snap-frozen in liquid nitrogen, and stored at −80°C. Cryosections (7 μm) were fixed in 4% paraformaldehyde for 10 min and incubated with 3% hydrogen peroxide for 15 min at room temperature. The sections were blocked with 1% BSA for 60 min and then incubated with either anti-mouse TNF-α MAb (BD Biosciences, Franklin Lakes, NJ), anti-mouse CD4 MAb (BD Biosciences), anti-mouse F4/80 MAb (eBioscience, San Diego, CA), or isotype-matched control Ig (BD Biosciences), at 4°C overnight followed by incubation with goat anti-rat Ig (Histofine Simple Stain MAX-PO, Nichirei Biosciences, Tokyo, Japan), for 30 min. The signals were visualized by diaminobenzidine (peroxidase substrate kit, Vector Laboratories, Burlingame, CA) and the sections were counterstained with hematoxylin. For immunofluorescence studies, the sections were stained with anti-β-catenin MAb (BD Biosciences) or anti-p-p65 PAb at serine 276 (Cell Signaling Technology) followed by incubation with Alexa^{594}-conjugated anti-mouse IgG1 or anti-rabbit IgG (Invitrogen) and DAPI (Vector Laboratory).

Statistical Analysis

Results were expressed as means ± SE. Statistics were determined by nonparametric Mann-Whitney *U*-test, and *P* values <0.05 were considered significant.

RESULTS

TNF-α Is Markedly Upregulated in the Inflamed Mucosa of DSS-Treated Mice

To first assess whether TNF-α is induced in the inflamed colonic tissue in C57BL/6 mice by administration of DSS, mice were administered 3.0% DSS-contained drinking water for 5 days (*days 0* to *5*, acute phase) followed by removal of DSS for another 2–5 days (recovery phase) with preinjection with AOM 7 days before starting DSS treatment (Fig. 1*A*). Total RNA was then isolated from the colon tissues of these mice. Consistent with previous report (37), we observed significantly increased level of TNF-α mRNA at *days 7* and *10* in DSS-treated mice compared with the control preinjected with AOM without DSS treatment (Fig. 1*B*). This observation was also confirmed by Western blotting (data not shown). Furthermore, immunohistochemistry revealed that the majority of TNF-α-expressing cells were located in the lamina propria and

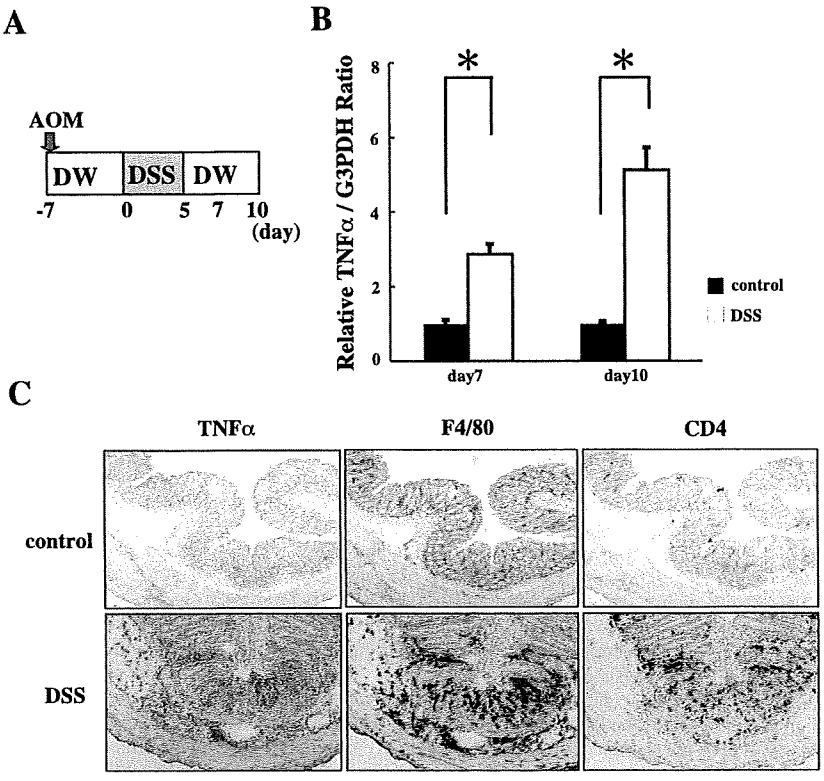

Fig. 1. TNF-α is profoundly induced in dextran sodium sulfate (DSS) colitis. *A*: protocol for acute DSS colitis. Mice were preinjected with 10 mg/kg of azoxymethane (AOM) or vehicle control 7 days before the start of DSS administration. DW, distilled water. *B*: relative mRNA expression of TNF-α in whole colon tissues that were taken from mice treated with control (regular water) or DSS at *days 7* and *10*. The levels of the mRNA were quantified by real-time PCR and normalized to the level of glyceraldehyde-3-phosphate dehydrogenase (G3PDH) ($n = 3$). *$P <$ 0.01. *C*: Immunohistochemistry. Frozen sections of colon tissues from control or DSS-treated mice at *day 10* were stained with anti-TNF-α, anti-CD4 or anti-F4/80 antibodies.

submucosa and some in the tunica muscularis (Fig. 1*C*). In addition, such TNF-α upregulation in DSS-treated colitis was not affected regardless of AOM preinjection (data not shown). Immunohistochemistry also revealed that the injured colonic tissues during the recovery phase were profoundly infiltrated by F4/80$^+$ macrophages as well as CD4$^+$ T cells compared with the untreated mice. Interestingly, the majority of TNF-α-expressing cells seemed to be macrophages rather than T cells (Fig. 1*C*). These results are consistent with the previous studies using BALB/c mice (37).

Administration of DSS Leads to Upregulation of TNFR2 but not TNFR1 in Colonic Epithelia

TNF-α-specific receptors composed of TNFR1 (p55) and 2 (p75) are known to be expressed in human intestinal epithelial cells and can be upregulated by IFN-γ (45, 49). Furthermore, it has been suggested that TNF-α is involved in the tissue repair of wounded epithelial layer (10). On the basis of the induction of TNF-α in colonic tissues by DSS treatment, TNFR1 and 2 protein expressions in colonic epithelial cells were predicted to be upregulated in this model. Therefore, we next assessed the expression levels of these molecules in the inflamed epithelial cells of AOM/DSS-treated mice. Primary colonic epithelial cells were isolated from the AOM-preinjected mice with or without DSS treatment described above at *day 10* (Fig. 1*A*). As expected, quantitative RT-PCR (Fig. 2*A*) and Western blotting (Fig. 2*B*) showed that colonic epithelial cells expressed endogenous low amount of both TNFR1 and 2. Notably, such expression of TNFR2, but not TNFR1, was significantly upregulated by DSS treatment (Fig. 2).

NF-κB Pathway, but not Death Domain Cascade, in Colonic Epithelial Cells Is Activated by DSS Treatment

It is suggested that the binding of TNF-α to TNFRs potentially results in the activation of two independent pathways, NF-κB and death domain (DD) (48). Given the result of TNFR2 upregulation in DSS colitis, we next assessed the activities of NF-κB and DD pathways in primary colonic epithelial cells from AOM/DSS-treated mice. As depicted in Fig. 3*A*, IκBα, which is upstream molecule of NF-κB, and p65/Rel A, one of the NF-κB components, were significantly activated in association with TNFR2 upregulation in AOM/DSS-treated colonic epithelia at *day 10*. In contrast, such treatment did not affect the expression of neither p-FADD nor cleaved (c)-caspase 3, a downstream molecule of DD, in these cells during the recovery phase (Fig. 3*B*).

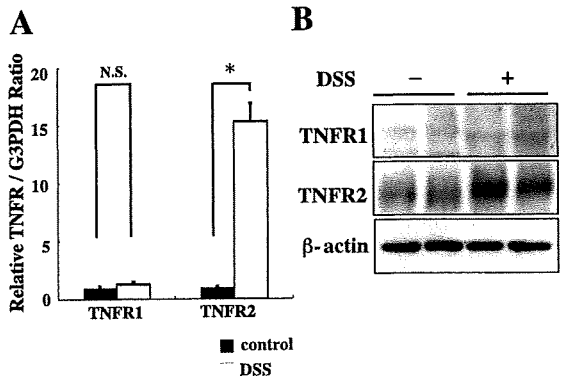

Fig. 2. TNF receptor (TNFR) 2 in colonic epithelia is upregulated in DSS colitis. *A*: relative mRNA expression levels of TNFR1 and 2 in colonic epithelial cells from mice treated with control (regular water) or DSS at *day 10*. The levels of the mRNAs were quantified by real-time PCR and normalized to the level of G3PDH (n = 3). *$P < 0.01$. *B*: protein lysates of isolated colonic epithelial cells from control- or DSS-treated mice at *day 10* were subjected to Western blotting with anti-TNFR1, anti-TNFR2, or anti-β-actin antibodies.

TNF-α Stimulates NF-κB Pathway in Intestinal Epithelial Cells

Given the upregulation of TNFR2 and specific activation of NF-κB, but not DD, in colonic epithelial cells in AOM/DSS colitis, we next utilized a mouse colonic epithelial cell line, CT26, to examine whether TNFR2 signaling is associated with NF-κB activation in these epithelial cells. CT26 cells were cultivated in the absence or presence of rIFN-γ to induce TNFRs upregulation. Although CT26 cells endogenously expressed TNFR2, its level was not upregulated in the presence of IFN-γ. This suggested that CT26 cells constitutively express maximum level of TNFR2 in the condition (data not shown). Moreover, we also observed that these cells express both p65 and IκBα (Fig. 4*A*). To further confirm whether TNFR2 in those cells is functional, the activation of NF-κB by rTNF-α was examined. Intestinal CT26 cells were stimulated with several concentrations of rTNF-α for 5 min. As shown in Fig. 4*A*, in vitro stimulation with rTNF-α led to the phosphorylation of p65 and IκBα in CT26 cells in a dose-dependent fashion.

Given the upregulated expression of TNFR2 and its signal profile in the stimulated-CT26 cells, we next examined the effect of anti-TNF-α MAb on NF-κB activation in these cells. CT26 cells were stimulated with 10 ng/ml of rTNF-α for 5 min in the presence of various concentrations of anti-TNF-α MAb, MP6-XT22. Although total expression level of p65 in rTNF-α-stimulated CT26 cells were not affected, phosphorylation of p65 in these cells was suppressed by the blockade of TNF-α with MP6-XT22 in a dose-dependent fashion (Fig. 4*B*). Similarly, neutralization of rTNF-α by MP6-XT22 also attenuated the phosphorylation status of IκBα in CT26 cells in a dose-dependent fashion. Furthermore, our kinetic assessment revealed that such suppression of NF-κB pathway by anti-TNF-α MAb did not express delayed signal response since both MP6-XT22-treated and control IgG-treated cells showed maximum level of p-p65 and p-IκBα around 10 min after the stimulation with rTNF-α (Fig. 4*C*). It should be noted that we consistently observed the degradation of IκBα 15 min after rTNF-α stimulation although the expressions of p-p65 and p-IκBα reach maximum level at 10 min. These results indicate that TNF-α stimulation against colonic epithelial cells results in activation of NF-κB via TNFR2 and, moreover, MP6-XT22 can arrest such activation.

Anti-TNF-α MAb Treatment Suppresses NF-κB Activation in Acute DSS Colitis Model

On the basis of the in vitro evidence of NF-κB inactivation by MP6-XT22 in rTNF-α-stimulated CT26 cells, we next confirmed this observation in the acute DSS colitis model to pursue more physiological function of MP6-XT22 in vivo. Because NF-κB is known to be critical in the induction of tissue inflammation such as colitis, it was initially anticipated that treatment with anti-TNF-α MAb would suppress the de-

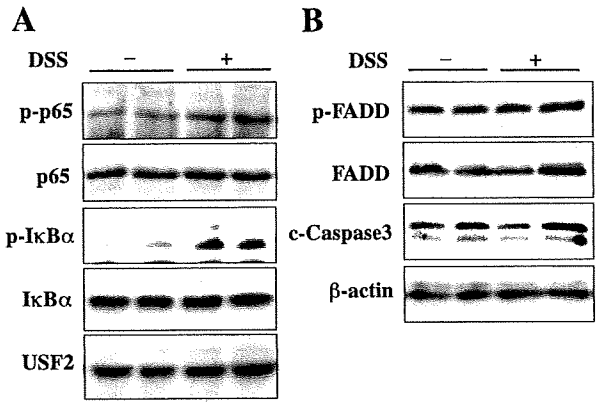

Fig. 3. NF-κB pathway in colonic epithelial cells is activated in DSS colitis. Protein lysates of isolated colonic epithelial cells from control or DSS-treated mice at *day 10* were subjected to Western blotting with either anti-p65, anti-p-p65, anti-IκBα, anti-p-IκBα, or anti-USF2 antibodies for the assessment of NF-κB activity (*A*) and anti-FADD, anti-p-FADD, anti-cleaved (c)-caspase 3, or anti-β-actin antibodies for apoptosis activity (*B*).

velopment of colitis. Therefore, we administered either control IgG or MP6-XT22 ip to the AOM/DSS-administered mice at *day 5* after DSS ingestion (Fig. 5*A*) followed by histological assessment at *days 7* and *10*. Then colonic epithelial cells were isolated at *day 10*. Unexpectedly, however, there was no significant difference in the histological score between two groups irrespective of administration of anti-TNF-α MAb or control IgG (Fig. 5*B*). On the other hand, AOM/DSS-treated epithelial samples with control IgG showed markedly upregulated p-IκBα and p-p65 expressions. However, injection with MP6-XT22 into AOM/DSS-treated mice resulted in suppression of IκBα and p65 phosphorylation, although total expression levels of p65 and IκBα were not affected in these samples (Fig. 5*C*). Given this discrepancy between the activities of NF-κB and the proportions of colitis in our experiments, we subsequently evaluated cytokine production such as IL-1β, IL-6, and MIP-2 (mouse homolog of human IL-8) in this model. Total RNA samples were extracted from colonic tissues of mice treated as above. Interestingly, quantitative RT-PCR analysis revealed significantly reduced mRNA expressions for IL-1β, IL-6, and MIP-2 in whole colons from MP6-XT22-treated mice at *day 7* compared with those of the control group (Fig. 5*D*). These results indicate that induced TNF-α in mucosal tissues may not be essential for colitis exacerbation but is somehow responsible for the production of these cytokine secondary to NF-κB activation in the DSS model.

Repetitive Anti-TNF-α MAb Treatment Suppresses Development of CAC in AOM/DSS-Treated Mice

The present protocol of anti-TNF-α MAb (MP6-XT22) administration has been useful in the assessment of TNF-α/TNFR signaling pathway on the development of CAC, because this does not affect the inflammation of DSS colitis but rather

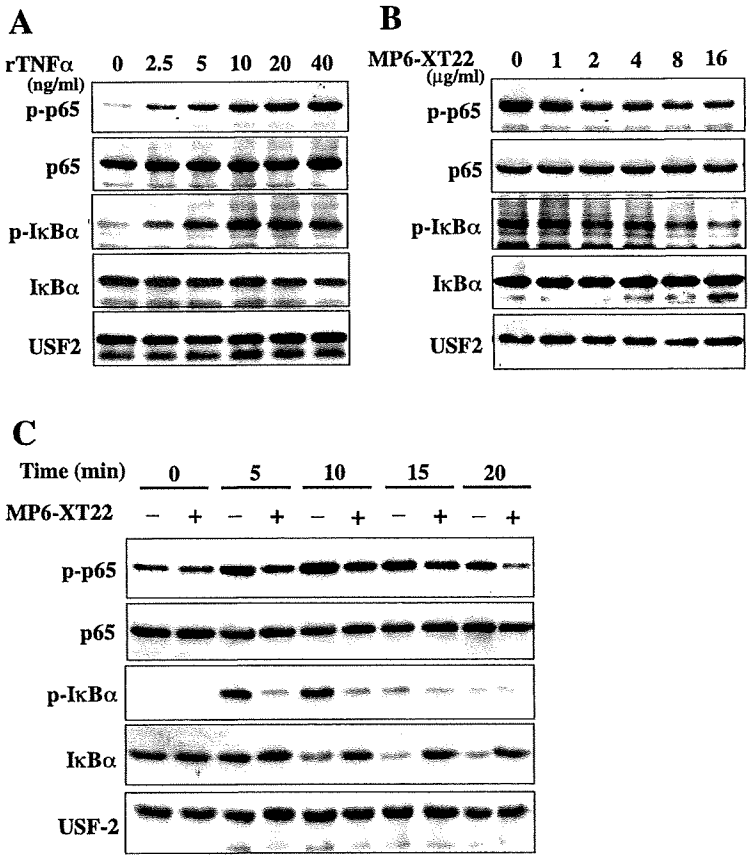

Fig. 4. MP6-XT22 suppresses NF-κB activation in TNF-α-stimulated CT26 cells. *A*: protein lysates from CT26 cells stimulated with indicated concentration of rTNF-α were subjected to Western blotting with anti-p65, anti-p-p65, anti-IκBα, anti-p-IκBα, or anti-USF2 antibodies. Representative data at 5 min after TNF-α-stimulation are shown. *B*: protein lysates from 10 ng/ml rTNF-α-stimulated CT26 cells incubated with the indicated concentration of MP6-XT22 were subjected to Western blotting with anti-p65, anti-p-p65 anti-IκBα, anti-p-IκBα, or anti-USF2 antibodies. Representative data at 5 min after TNF-α-stimulation are shown. *C*. protein lysates from CT26 cells incubated with either control IgG or MP6-XT22 (10 μg/ml) with rTNF-α (10 ng/ml) stimulation at the indicated time point were subjected to Western blotting with anti-p65, anti-p-p65 anti-IκBα, anti-p-IκBα, or anti-USF2 antibodies.

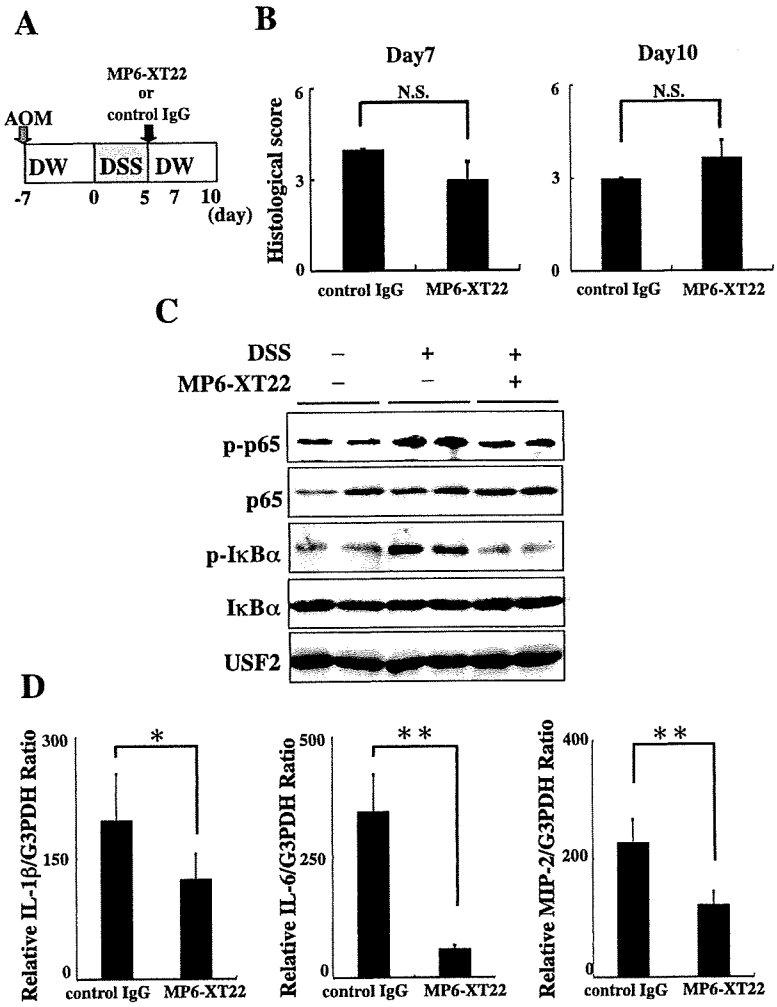

Fig. 5. MP6-XT22 treatment diminishes NF-κB activity in DSS-treated colonic epithelial cells, but it does not ameliorate severity of colitis. *A*: protocol for acute DSS colitis. Mice received MP6-XT22 or control IgG (1 mg/mouse) at *day 5*. *B*: histological scores at *day 7* ($n = 3$) and *day 10* ($n = 6$) are shown. Data are expressed as means ± SE. *C*, protein lysates of isolated colonic epithelial cells from control or DSS-treated mice at *day 10* with or without MP6-XT22 injection were subjected to Western blotting with anti-IκBα, anti-p-IκBα, anti-p65, anti-p-p65, or anti-USF2 antibodies. *D*: relative mRNA expressions for IL-1β, IL-6 and MIP-2 in whole colons from mice treated with control IgG or MP6-XT22 injection at *day 10*. Each mRNA level was quantified by real-time PCR and normalized to the level of G3PDH ($n = 3$). $^*P < 0.01$, $^{**}P < 0.05$.

suppress activation of NF-κB in epithelial cells. Therefore, this excludes the possibility that different degree of inflammation by the treatment secondarily affect the development of CAC. Thus we next investigated whether repetitive administration anti-TNF-α MAb suppresses the development of CAC in AOM/DSS-treated mice. Mice received AOM IP at *day −7*, followed by three cycles of DSS treatment and weekly injection of either control IgG or MP6-XT22 from *day 5* until *day 68*. These mice were then euthanized on *day 70* (see Fig. 6*A*). Consistent with acute model of DSS colitis as mentioned above, both groups of mice showed similar severity of clinical phenotypes as determined by weight loss, rectal bleeding, and diarrhea regardless of the treatments with MP6-XT22 (Fig. 6*B*). Histological findings of crypt destruction, mucosal ulceration, and infiltration were similarly observed in both groups of mice in association with the clinical scores of these mice (Fig. 6*C*). It should be noted that clinical and histological scores showed that the severity of inflammation was not affected by AOM treatment (data not shown).

It has been recently reported that NF-κB activation in epithelial cells and myeloid cells plays a crucial role in carcinogenesis (12). Thus it was suggested that blockade of TNF-α may be effective for incidence and/or progression of tumors. Therefore, we investigated the effect of anti-TNF-α MAb on the development of colitis-associated tumors in chronic DSS/AOM model. Mice administered with combination of AOM, DSS, and control IgG showed development of multiple nodular or polyploid tumors in the middle to distal colon (Fig. 7*A*). In contrast, decreased number of tumors was observed in mice administered with the combination of AOM, DSS, and MP6-XT22 (Fig. 7, *A* and *B*). Moreover, MP6-XT22 treatment also decreased the numbers of small tumors as well as larger tumors (Fig. 7*C*), despite similar morphological diversity in both groups (Fig. 7*D*), suggesting that the suppressed tumorigenesis in MP6-XT22-treated group is not only due to the reduced progression of tumors. Next, we thoroughly examined the histological sections, and no evidence of carcinoma such as tumor invasion into the lamina propria was observed in both control IgG and MP6-XT22 treated groups. Therefore, we defined the histology of this colitis-associated tumor model as adenoma. In addition, we also examined the β-catenin expression in these sections. The expression of β-catenin was observed in the cytoplasm, but not in the nuclei, of intestinal epithelia with colitis, as seen in Fig. 7*E*. However, the tumor

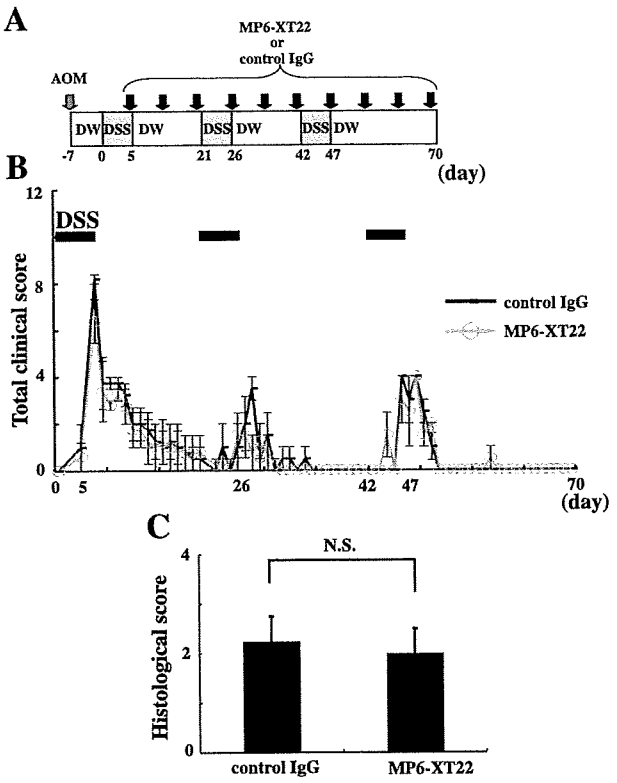

Fig. 6. MP6-XT22 does not ameliorate chronic DSS colitis. *A*: schema of the AOM/DSS colitis-associated tumor model. Mice were preinjected with AOM 7 days before starting DSS administration, and subsequently administered weekly injections of MP6-XT22 or isotype control from *day 5* until day 68 during the three cycles of DSS administration. *B* and *C*: clinical (*B*) and histological (*C*) scores are shown. Data (n = 10) are expressed as means ± SE. N.S., not significant.

cells showed the nuclear expression of β-catenin as well as its overexpression in the cytoplasm (Fig. 7*E*). Given the nuclear translocation of β-catenin in our tumor model (Fig. 7*E*) and the attenuation of tumor development by anti-TNF-α therapy (Fig. 7, *A–C*), we next examined TNFR2 expression as well as NF-κB activities in this model. Interestingly, TNFR2 expression was more upregulated in the colitis-associated tumor. In addition, the phosphorylation of IκBα and p65 was further induced in the tumors in association with the upregulation of TNFR2 (Fig. 7*F*). These studies indicate that the NF-κB activation via TNFR2 in intestinal epithelial cells is closely associated with epithelial tumorigenesis. Moreover, we also observed that the nuclear expression of p65 was induced in the epithelia in tumor

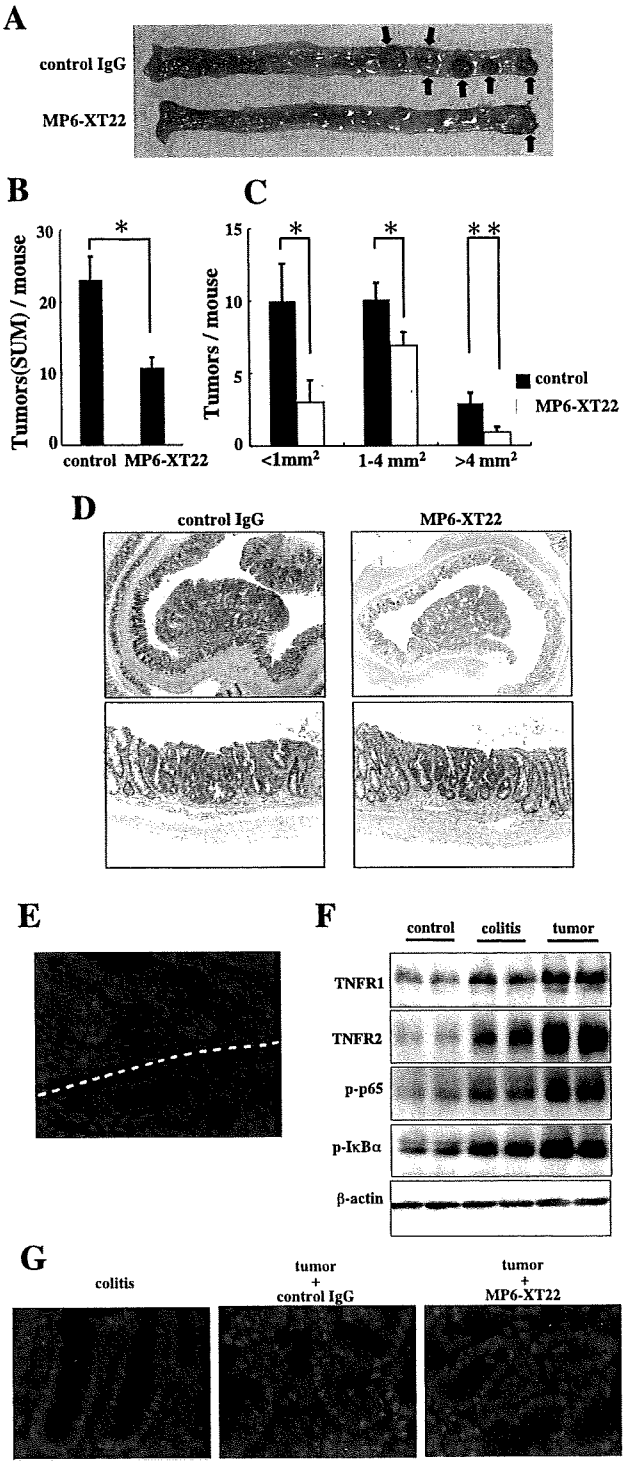

Fig. 7. MP6-XT22 reduces tumor development in AOM/DSS model. *A*: macroscopic overview of representative colonic samples from each group is shown. Arrows indicate tumors. *B*: numbers of microscopically indicated tumors per colon in AOM/DSS-administered mice with isotype control or MP6-XT22 treatment (n = 10). Data are express as means ± SE. $^*P < 0.01$, $^{**}P < 0.05$. *C*: histogram shows tumor size distribution. Tumors were determined under the microscope. *D*: microscopic morphology of AOM/DSS tumor model. Representative histological sections with hematoxylin and eosin staining from each group are shown. *E*: β-catenin expression in colitis-associated cancer (CAC). Cryosections from AOM/DSS-treated mice were stained with anti-β-catenin MAb and anti-mouse IgG1-Alexa^{594}. Representative sample at *day 70* is shown. *Top*, tumor area; *bottom*, nontumor area. *F*: protein lysates of isolated epithelial cells from nontreated control, colitis or tumor tissues were subjected to Western blotting with anti-TNFR1, anti-TNFR2, anti-p-p65, anti-p-IκBα or anti-β-actin antibodies. *G*: cryosections of colon tissues of healthy control, colitis, CAC with control IgG or CAC with MP6-XT22 treatment were stained with anti-p-p65 PAb and anti-rabbit IgG-Alexa^{594}.

tissues. However, such nuclear translocation of p65 was significantly suppressed by MP6-XT22 treatment (Fig. 7*G*). These findings indicate that blockade of TNF-α may contribute to suppressed initiation of colitis-associated tumors in our AOM/DSS model as well as reduction of tumor progression.

DISCUSSION

Our studies showed that blockade of TNF-α in vivo did not affect the severity of DSS-induced inflammation but rather reduced the development and progression of CAC. It has been recently reported by another group that reduced inflammation in TNFR1-deficient mice may contribute to the suppression of CAC (37). However, our results suggest that continuous suppression of TNF-α activity by MAb injection for patients with IBD, even if they are refractory to anti-TNF-α therapy, may reduce the risk of CAC.

TNF-α is a pivotal cytokine in the pathogenesis of IBD since anti-TNF-α MAb therapy is used as a powerful and promising treatment for patients with CD (13, 41, 44) or UC (40) in recent years. It has been also reported that the anti-TNF-α treatment is also effective therapy in several animal models of colitis such as TNBS colitis model, $CD4^+CD45RB^{high}$ T cell-reconstituted model, bone marrow transplanted tgε 26 model, and Cottontop tamarin model (24, 30, 38). Interestingly, however, the effect of TNF-α MAb therapy is controversial in the DSS colitis model, which is an epithelial damage model rather than a T cell-mediated model. For example, it has been reported that anti-TNF-α antibody treatment can ameliorate acute and chronic DSS-induced colitis (20, 28). Moreover, multiple injections of anti-TNF-α Ab during the process of chronic DSS reduced the disease activity and cytokine productions in the first two cycles although adverse effects were observed in the third cycle of the DSS treatment (27). However, other groups have reported that the antibody therapy against TNF-α failed to suppress the severity of colitis in this model (20, 33). Moreover, it has been reported that DSS-induced inflammation was significantly enhanced in TNF-α deficient-animals (29). This observation is somewhat similar to our results since anti-TNF-α treatment did not affect the clinical symptoms and pathological studies. Since the wounded epithelial layer by DSS treatment results in the translocation of luminal bacteria into the intestinal mucosa in this model, one of the potential interpretations regarding the different observations by others and ours is that in the setting of inflammation in acute and/or chronic DSS colitis, environmental effect such as the different microflora in different animal facilities may explain the discrepancy among the above results. Another interpretation might be that the colitis model in our studies was relatively mild compared with the others' and therefore we did not observe explicit abrogation of colitis by anti-TNF MAb administration.

Secreted TNF-α molecules in inflamed tissues can be recognized by its specific receptors such as TNFR1 and 2, which are known to be expressed in several cell types including macrophages and intestinal epithelial cells. The cytoplasmic domains of TNFR1 and 2 are known to be associated with TRAF2 by which activation of IKK is induced. Subsequently, activated IKK induces phosphorylation of IκB, resulting in activation of NF-κB, which consists of p50 and Rel A/p65, due to dissociation of IκB/NF-κB complex. In addition to NF-κB activation, however, TNFR1 is also capable of being recruited by FADD and TNFR-associated DD protein (TRADD) by TNF-α activation. The oligomerization of such molecules induces activation of cysteine proteases such as caspase 8, resulting in apoptosis. Interestingly, however, TNFR2, which is not coupled with FADD/TRADD complex, does not induce proapoptotic signaling when interacting with TNF-α. In this regard, we observed that TNFR2 is preferentially upregulated in regenerating epithelial cells in DSS colitis. Our interpretation of these results are that intestinal epithelial cells, when rapidly expanding, is associated with the expression of TNFR2 rather than TNFR1, and thus counter that of the proapoptotic signals of intestinal epithelia. Consistent with this, we also observed specific activation of IκB and p65 in association with TNFR2 upregulation in wounded mucosal epithelia by DSS administration. Thus it is suggested that regenerating intestinal epithelial cells may have susceptibility of NF-κB inactivation by blockade of TNF-α due to the specific upregulation of TNFR2 in these cells.

It is well known that long-standing UC (8, 18, 25) and CD (4, 7) are closely associated with an increased risk of CAC. To investigate the role of TNF-α signaling in colon carcinogenesis, we here used an established murine CAC model based on the mutagenic agent AOM (32, 43) along with the colitogenic administration of DSS. It has been suggested by Greten and colleagues (12) that IKK-β contributes to tumor promotion in AOM/DSS-induced CAC model. They indicated that the deletion of IKK-β in myeloid cells or epithelial cells resulted in decreased size of tumors due to reduced expression of proinflammatory cytokines that may serve as tumor growth factors (12). Moreover, it has been reported that blockade of IL-6 prevents tumor progression in AOM/DSS-induced CAC model (3). In addition, Popivanova and colleagues (37) have recently reported that the TNFR1 signaling in hematopoietic cells in colonic tissues results in production of chemokines such as CXCL1 and CCL2, which are chemotactic for neutrophils and macrophages. They also suggested that such activation of hematopoietic cells in the mucosal tissue is critical for the progression of CAC in association with suppression of DSS colitis. In our studies, colitis was mild and not clearly affected by anti-TNF-α MAb treatment despite the depressed CAC initiation and progression observed. One of the interpretations regarding different observations is that TNFR1 deficient neutrophils and macrophages on the BALB/c background may have different immunological context from that of our model on the C57BL/6 background. Some of our observation is consistent with these, because blockade of TNF-α in chronic DSS colitis by treatment with MP6-XT22 resulted in decreased cytokine expression including IL-1β, IL-6, and MIP-2, which are considered to encourage protumorigenic activities such as angiogenesis and tumor proliferation (5, 6, 19, 21). Thus it is suggested that the blockade of TNF-α may function to suppress the secretion of these chemokines and cytokines from infiltrating lymphocytes in colitic tissue through the inhibition of NK-κB activity in these cells. It should be noted that anti-TNF-α MAb treatment is also effective for suppression of tumorigenesis in unique mouse CAC model, which is promoted by transferring of $CD4^+CD45RB^{high}$ lymphocytes that may produce proinflammatory cytokine into Apc (Min/+) mice (39). This might be another evidence for the proinflammatory cytokine-induced epithelial carcinogenesis.

On the other hand, it was also suggested by Greten and colleagues (12) that deletion of IKK-β in intestinal epithelial cells led to a decrease in tumor incidence although inflammation in the tissue was not abrogated. Consistent with this, it was also suggested by another group that inactivation of NF-κB in the hepatocytes had no effect during the course of hepatitis but failed to progress to carcinoma in an animal model of hepatitis-induced hepatocellular carcinoma (36). Although the amelioration of colitis was not apparent in our study, anti-TNF-α Ab significantly suppressed the tumor development in our AOM/DSS model in association with the downregulation of p-p65 and p-IκB. Thus our results are consistent with observations by others above since treatment with MP6-XT22 resulted in the reduction of TNF-α-induced NF-κB activity in colonic epithelial cells, which may influence the cell growth of colonic epithelia in DSS colitis. Regarding the involvement of apoptosis, we have tried to detect p-FADD and c-caspase 3 expressions in DSS-receiving mice, but we did not observe any significant differences compared with nontreated controls, as seen in Fig. 3*B*. Moreover, we have also tried to detect DNA fragmentation from rTNF-α-stimulated CT26 cells as well as TUNEL staining in the setting of recovery phase of DSS-treated or AOM/DSS-treated mice with or without anti-TNF-α treatment. However, we were not able to observe any significant difference of apoptosis activities in these experiments compared with the controls (data not shown). Therefore, we conclude that apoptosis is unlikely to be associated with the development of our colitis-associated tumor model. Moreover, we have also observed that the NF-κB pathway is further activated in CAC tissues compared with nontumor tissues in DSS/AOM-receiving mice in association with nuclear expression of β-catenin (Fig. 7*E*) and extraordinary upregulation of TNFR2 (Fig. 7*F*). These observations evidently imply that NF-κB activation via TNFR2 in the intestinal epithelial cells is directly correlated with the carcinogenesis induced by TNF-α stimulation. Thus it should be clarified that TNFR2 signaling in intestinal epithelia is also required for such tumor promotion as well as TNFR1 signaling in hematopoietic cells. We have therefore tried to focus on addressing this issue by using a "conventional" TNFR2-deficient model. We administered AOM and DSS treatment to these mice; however, we were not able to quantify and compare tumor development in such mice, because these mice were more sensitive to DSS colitis and had higher mortality compared with WT mice (data not shown). Our interpretation of this result is that serum TNF-α levels in conventional TNFR2-deficient mice may be elevated with LPS stimulation as previously reported by other group (35). We therefore realized that an "intestinal epithelia-specific" deficient model rather than conventional knockout mice would likely be the better model for our study. However, we were not able to obtain such conditional deficient mice. On the other hand, Fukata and colleagues (11) have recently reported that impaired Toll-like receptor-4 (TLR4) signaling reduced AOM/DSS-induced colon cancer without significant impact on inflammation. Their findings and ours may imply an important mechanism by which NF-κB pathway is regulated in intestinal epithelial cells in setting of carcinogenesis. Thus one potential mechanism by which anti-TNF-α MAb is able to reduce the numbers and size of tumors in AOM/DSS-administered mice is that blocking TNFR2 signaling, which was presumably triggered by TLR4-mediated epithelial stimulation, in the context of chronic intestinal wound healing may somehow decrease neoplasia even without significantly impairing inflammation. In addition, we have also observed that TNFR2 signaling in colonic epithelial cells results in the epithelial barrier dysfunction (M. Onizawa and T. Nagaishi, unpublished data). This observation suggests that TNFR2 signaling-mediated impairment of epithelial tight junction may be associated with the mechanism of tumor development.

In summary, administration of anti-TNF-α MAb directly inhibits NF-κB activities in intestinal epithelial cells that may induce tumor formation in collaboration with independent mechanisms by another NF-κB activity in the hematopoietic cells. Although more detail mechanism still remains to be elucidated, distinct TNF-α signaling in colonic epithelial cells may be one potential therapeutic target in the treatment of IBD-associated tumorigenesis, resulting in the change of natural history of patients with IBD.

ACKNOWLEDGMENTS

The authors thank Drs. Emiko Mizoguchi and Timothy Kuo for helpful discussions on this study.

GRANTS

This study was supported in part by grants-in-aid for Scientific Research, Scientific Research on Priority Areas, Exploratory Research and Creative Scientific Research from the Japanese Ministry of Education, Culture, Sports, Science and Technology; the Japanese Ministry of Health, Labor and Welfare; the Japan Medical Association; Foundation for Advancement of International Science; Terumo Life Science Foundation; Ohyama Health Foundation; Yakult Bio-Science Foundation; Research Fund of Mitsukoshi Health and Welfare Foundation; Japan Foundation for Applied Enzymology; Memorial Fund of Nihon University Medical Alumni Association; Abbott Japan Allergy Research Award; and Takeda Science Foundation.

REFERENCES

1. **Abrams JS, Roncarolo MG, Yssel H, Andersson U, Gleich GJ, Silver JE.** Strategies of anti-cytokine monoclonal antibody development: immunoassay of IL-10 and IL-5 in clinical samples. *Immunol Rev* 127: 5–24, 1992.
2. **Araki A, Kanai T, Ishikura T, Makita S, Uraushihara K, Iiyama R, Totsuka T, Takeda K, Akira S, Watanabe M.** MyD88-deficient mice develop severe intestinal inflammation in dextran sodium sulfate colitis. *J Gastroenterol* 40: 16–23, 2005.
3. **Becker C, Fantini MC, Schramm C, Lehr HA, Wirtz S, Nikolaev A, Burg J, Strand S, Kiesslich R, Huber S, Ito H, Nishimoto N, Yoshizaki K, Kishimoto T, Galle PR, Blessing M, Rose-John S, Neurath MF.** TGF-beta suppresses tumor progression in colon cancer by inhibition of IL-6 trans-signaling. *Immunity* 21: 491–501, 2004.
4. **Bernstein CN, Blanchard JF, Kliewer E, Wajda A.** Cancer risk in patients with inflammatory bowel disease: a population-based study. *Cancer* 91: 854–862, 2001.
5. **Coussens LM, Werb Z.** Inflammation and cancer. *Nature* 420: 860–867, 2002.
6. **Driscoll KE, Hassenbein DG, Howard BW, Isfort RJ, Cody D, Tindal MH, Suchanek M, Carter JM.** Cloning, expression, and functional characterization of rat MIP-2: a neutrophil chemoattractant and epithelial cell mitogen. *J Leukoc Biol* 58: 359–364, 1995.
7. **Ekbom A, Helmick C, Zack M, Adami HO.** Increased risk of large-bowel cancer in Crohn's disease with colonic involvement. *Lancet* 336: 357–359, 1990.
8. **Ekbom A, Helmick C, Zack M, Adami HO.** Ulcerative colitis and colorectal cancer. A population-based study. *N Engl J Med* 323: 1228–1233, 1990.
9. **Ekbom A, Helmick CG, Zack M, Holmberg L, Adami HO.** Survival and causes of death in patients with inflammatory bowel disease: a population-based study. *Gastroenterology* 103: 954–960, 1992.
10. **Feiken E, Romer J, Eriksen J, Lund LR.** Neutrophils express tumor necrosis factor-alpha during mouse skin wound healing. *J Invest Dermatol* 105: 120–123, 1995.

11. **Fukata M, Chen A, Vamadevan AS, Cohen J, Breglio K, Krishnareddy S, Hsu D, Xu R, Harpaz N, Dannenberg AJ, Subbaramaiah K, Cooper HS, Itzkowitz SH, Abreu MT.** Toll-like receptor-4 promotes the development of colitis-associated colorectal tumors. *Gastroenterology* 133: 1869–1881, 2007.
12. **Greten FR, Eckmann L, Greten TF, Park JM, Li ZW, Egan LJ, Kagnoff MF, Karin M.** IKKbeta links inflammation and tumorigenesis in a mouse model of colitis-associated cancer. *Cell* 118: 285–296, 2004.
13. **Hanauer SB, Feagan BG, Lichtenstein GR, Mayer LF, Schreiber S, Colombel JF, Rachmilewitz D, Wolf DC, Olson A, Bao W, Rutgeerts P.** Maintenance infliximab for Crohn's disease: the ACCENT I randomised trial. *Lancet* 359: 1541–1549, 2002.
14. **Itzkowitz SH.** Cancer prevention in patients with inflammatory bowel disease. *Gastroenterol Clin North Am* 31: 1133–1144, 2002.
15. **Kanai T, Totsuka T, Uraushihara K, Makita S, Nakamura T, Koganei K, Fukushima T, Akiba H, Yagita H, Okumura K, Machida U, Iwai H, Azuma M, Chen L, Watanabe M.** Blockade of B7-H1 suppresses the development of chronic intestinal inflammation. *J Immunol* 171: 4156–4163, 2003.
16. **Karhausen J, Furuta GT, Tomaszewski JE, Johnson RS, Colgan SP, Haase VH.** Epithelial hypoxia-inducible factor-1 is protective in murine experimental colitis. *J Clin Invest* 114: 1098–1106, 2004.
17. **Karin M, Cao Y, Greten FR, Li ZW.** NF-kappaB in cancer: from innocent bystander to major culprit. *Nature Rev* 2: 301–310, 2002.
18. **Karlen P, Lofberg R, Brostrom O, Leijonmarck CE, Hellers G, Persson PG.** Increased risk of cancer in ulcerative colitis: a population-based cohort study. *Am J Gastroenterol* 94: 1047–1052, 1999.
19. **Koch AE, Polverini PJ, Kunkel SL, Harlow LA, DiPietro LA, Elner VM, Elner SG, Strieter RM.** Interleukin-8 as a macrophage-derived mediator of angiogenesis. *Science* 258: 1798–1801, 1992.
20. **Kojouharoff G, Hans W, Obermeier F, Mannel DN, Andus T, Scholmerich J, Gross V, Falk W.** Neutralization of tumour necrosis factor (TNF) but not of IL-1 reduces inflammation in chronic dextran sulphate sodium-induced colitis in mice. *Clin Exp Immunol* 107: 353–358, 1997.
21. **Lahm H, Petral-Malec D, Yilmaz-Ceyhan A, Fischer JR, Lorenzoni M, Givel JC, Odartchenko N.** Growth stimulation of a human colorectal carcinoma cell line by interleukin-1 and -6 and antagonistic effects of transforming growth factor beta 1. *Eur J Cancer* 28A: 1894–1899, 1992.
22. **Li Q, Verma IM.** NF-kappaB regulation in the immune system. *Nat Rev Immunol* 2: 725–734, 2002.
23. **MacDonald TT, Monteleone G, Pender SL.** Recent developments in the immunology of inflammatory bowel disease. *Scand J Immunol* 51: 2–9, 2000.
24. **Mackay F, Browning JL, Lawton P, Shah SA, Comiskey M, Bhan AK, Mizoguchi E, Terhorst C, Simpson SJ.** Both the lymphotoxin and tumor necrosis factor pathways are involved in experimental murine models of colitis. *Gastroenterology* 115: 1464–1475, 1998.
25. **Mellemkjaer L, Olsen JH, Frisch M, Johansen C, Gridley G, McLaughlin JK.** Cancer in patients with ulcerative colitis. *Int J Cancer* 60: 330–333, 1995.
26. **Moore RJ, Owens DM, Stamp G, Arnott C, Burke F, East N, Holdsworth H, Turner L, Rollins B, Pasparakis M, Kollias G, Balkwill F.** Mice deficient in tumor necrosis factor-alpha are resistant to skin carcinogenesis. *Nat Med* 5: 828–831, 1999.
27. **Murthy S, Cooper HS, Yoshitake H, Meyer C, Meyer CJ, Murthy NS.** Combination therapy of pentoxifylline and TNFalpha monoclonal antibody in dextran sulphate-induced mouse colitis. *Aliment Pharmacol Ther* 13: 251–260, 1999.
28. **Myers KJ, Murthy S, Flanigan A, Witchell DR, Butler M, Murray S, Siwkowski A, Goodfellow D, Madsen K, Baker B.** Antisense oligonucleotide blockade of tumor necrosis factor-alpha in two murine models of colitis. *J Pharmacol Exp Ther* 304: 411–424, 2003.
29. **Naito Y, Takagi T, Handa O, Ishikawa T, Nakagawa S, Yamaguchi T, Yoshida N, Minami M, Kita M, Imanishi J, Yoshikawa T.** Enhanced intestinal inflammation induced by dextran sulfate sodium in tumor necrosis factor-alpha deficient mice. *J Gastroenterol Hepatol* 18: 560–569, 2003.
30. **Neurath MF, Fuss I, Pasparakis M, Alexopoulou L, Haralambous S, Meyer zum Buschenfelde KH, Strober W, Kollias G.** Predominant pathogenic role of tumor necrosis factor in experimental colitis in mice. *Eur J Immunol* 27: 1743–1750, 1997.
31. **Nielsen OH, Vainer B, Madsen SM, Seidelin JB, Heegaard NH.** Established and emerging biological activity markers of inflammatory bowel disease. *Am J Gastroenterol* 95: 359–367, 2000.
32. **Okayasu I, Ohkusa T, Kajiura K, Kanno J, Sakamoto S.** Promotion of colorectal neoplasia in experimental murine ulcerative colitis. *Gut* 39: 87–92, 1996.
33. **Olson AD, DelBuono EA, Bitar KN, Remick DG.** Antiserum to tumor necrosis factor and failure to prevent murine colitis. *J Pediatr Gastroenterol Nutr* 21: 410–418, 1995.
34. **Oshima S, Nakamura T, Namiki S, Okada E, Tsuchiya K, Okamoto R, Yamazaki M, Yokota T, Aida M, Yamaguchi Y, Kanai T, Handa H, Watanabe M.** Interferon regulatory factor 1 (IRF-1) and IRF-2 distinctively up-regulate gene expression and production of interleukin-7 in human intestinal epithelial cells. *Mol Cell Biol* 24: 6298–6310, 2004.
35. **Peschon JJ, Torrance DS, Stocking KL, Glaccum MB, Otten C, Willis CR, Charrier K, Morrissey PJ, Ware CB, Mohler KM.** TNF receptor-deficient mice reveal divergent roles for p55 and p75 in several models of inflammation. *J Immunol* 160: 943–952, 1998.
36. **Pikarsky E, Porat RM, Stein I, Abramovitch R, Amit S, Kasem S, Gutkovich-Pyest E, Urieli-Shoval S, Galun E, Ben-Neriah Y.** NF-kappaB functions as a tumour promoter in inflammation-associated cancer. *Nature* 431: 461–466, 2004.
37. **Popivanova BK, Kitamura K, Wu Y, Kondo T, Kagaya T, Kaneko S, Oshima M, Fujii C, Mukaida N.** Blocking TNF-alpha in mice reduces colorectal carcinogenesis associated with chronic colitis. *J Clin Invest* 118: 560–570, 2008.
38. **Powrie F, Leach MW, Mauze S, Menon S, Caddle LB, Coffman RL.** Inhibition of Th1 responses prevents inflammatory bowel disease in scid mice reconstituted with CD45RBhi CD4+ T cells. *Immunity* 1: 553–562, 1994.
39. **Rao VP, Poutahidis T, Ge Z, Nambiar PR, Horwitz BH, Fox JG, Erdman SE.** Proinflammatory CD4+ CD45RB(hi) lymphocytes promote mammary and intestinal carcinogenesis in Apc(Min/+) mice. *Cancer Res* 66: 57–61, 2006.
40. **Rutgeerts P, Sandborn WJ, Feagan BG, Reinisch W, Olson A, Johanns J, Travers S, Rachmilewitz D, Hanauer SB, Lichtenstein GR, de Villiers WJ, Present D, Sands BE, Colombel JF.** Infliximab for induction and maintenance therapy for ulcerative colitis. *N Engl J Med* 353: 2462–2476, 2005.
41. **Sands BE, Anderson FH, Bernstein CN, Chey WY, Feagan BG, Fedorak RN, Kamm MA, Korzenik JR, Lashner BA, Onken JE, Rachmilewitz D, Rutgeerts P, Wild G, Wolf DC, Marsters PA, Travers SB, Blank MA, van Deventer SJ.** Infliximab maintenance therapy for fistulizing Crohn's disease. *N Engl J Med* 350: 876–885, 2004.
42. **Szlosarek P, Charles KA, Balkwill FR.** Tumour necrosis factor-alpha as a tumour promoter. *Eur J Cancer* 42: 745–750, 2006.
43. **Tanaka T, Kohno H, Suzuki R, Yamada Y, Sugie S, Mori H.** A novel inflammation-related mouse colon carcinogenesis model induced by azoxymethane and dextran sodium sulfate. *Cancer Sci* 94: 965–973, 2003.
44. **Targan SR, Hanauer SB, van Deventer SJ, Mayer L, Present DH, Braakman T, DeWoody KL, Schaible TF, Rutgeerts PJ.** A short-term study of chimeric monoclonal antibody cA2 to tumor necrosis factor alpha for Crohn's disease. Crohn's Disease cA2 Study Group. *N Engl J Med* 337: 1029–1035, 1997.
45. **Taylor CT, Dzus AL, Colgan SP.** Autocrine regulation of epithelial permeability by hypoxia: role for polarized release of tumor necrosis factor alpha. *Gastroenterology* 114: 657–668, 1998.
46. **Totsuka T, Kanai T, Iiyama R, Uraushihara K, Yamazaki M, Okamoto R, Hibi T, Tezuka K, Azuma M, Akiba H, Yagita H, Okumura K, Watanabe M.** Ameliorating effect of anti-inducible costimulator monoclonal antibody in a murine model of chronic colitis. *Gastroenterology* 124: 410–421, 2003.
47. **Totsuka T, Kanai T, Uraushihara K, Iiyama R, Yamazaki M, Akiba H, Yagita H, Okumura K, Watanabe M.** Therapeutic effect of anti-OX40L and anti-TNF-αlpha MAbs in a murine model of chronic colitis. *Am J Physiol Gastrointest Liver Physiol* 284: G595–G603, 2003.
48. **Wajant H, Pfizenmaier K, Scheurich P.** Tumor necrosis factor signaling. *Cell Death Differ* 10: 45–65, 2003.
49. **Wang F, Schwarz BT, Graham WV, Wang Y, Su L, Clayburgh DR, Abraham C, Turner JR.** IFN-gamma-induced TNFR2 expression is required for TNF-dependent intestinal epithelial barrier dysfunction. *Gastroenterology* 131: 1153–1163, 2006.
50. **Wang M, Bronte V, Chen PW, Gritz L, Panicali D, Rosenberg SA, Restifo NP.** Active immunotherapy of cancer with a nonreplicating recombinant fowlpox virus encoding a model tumor-associated antigen. *J Immunol* 154: 4685–4692, 1995.

Biochemical and Biophysical Research Communications 385 (2009) 230–235

Contents lists available at ScienceDirect

Biochemical and Biophysical Research Communications

journal homepage: www.elsevier.com/locate/ybbrc

Bioactivity-guided screening identifies pheophytin a as a potent anti-hepatitis C virus compound from Lonicera hypoglauca Miq.

Sheng-Yang Wang [a,1], Ching-Ping Tseng [b,1], Keng-Chang Tsai [c,2], Chia-Fan Lin [d,2], Ching-Ya Wen [d], Hsin-Sheng Tsay [e], Naoya Sakamoto [f], Chin-Hsiao Tseng [g,h], Ju-Chien Cheng [d,*]

[a] Department of Forestry, National Chung Hsing University, Taichung 402, Taiwan, ROC
[b] Graduate Institute of Medical Biotechnology, Chang Gung University, Taoyuan 333, Taiwan, ROC
[c] The Genomics Research Center, Academia Sinica, Taipei 115, Taiwan, ROC
[d] Department of Medical Laboratory Science and Biotechnology, China Medical University, Taichung 404, Taiwan, ROC
[e] Graudate Institute of Biochemical Sciences and Technology, Chaoyang University of Technology, Taichung 413, Taiwan, ROC
[f] Department of Gastroenterology and Hepatology, Tokyo Medical and Dental University, Tokyo, Japan
[g] Department of Internal Medicine, National Taiwan University Hospital and College of Medicine, Taipei 100, Taiwan, ROC
[h] Department of Medical Research and Development, National Taiwan University Hospital Yun-Lin Branch, Yun-Lin, Taiwan, ROC

ARTICLE INFO

Article history:
Received 26 April 2009
Available online 19 May 2009

Keywords:
Hepatitis C virus
Lonicera hypoglauca Miq.
Pheophytin a
Replicon cells

ABSTRACT

Chronic hepatitis C virus (HCV) infection is a worldwide public issue. In this study, we performed bioactivity-guided screening of the *Lonicera hypoglauca* Miq. crude extracts to find for naturally chemical entities with anti-HCV activity. Pheophytin a was identified from the ethanol-soluble fraction of *L. hypoglauca* that elicited dose-dependent inhibition of HCV viral proteins and RNA expression in both replicon cells and cell culture infectious system. Computational modeling revealed that pheophytin a can bind to the active site of HCV-NS3, suggesting that NS3 is a potent molecular target of pheophytin a. Biochemical analysis further revealed that pheophytin a inhibited NS3 serine protease activity with $IC_{50} = 0.89$ μM. Notably, pheophytin a and IFNα-2a elicited synergistic anti-HCV activity in replicon cells with no significant cytotoxicity. This study thereby demonstrates for the first time that pheophytin a is a potent HCV-NS3 protease inhibitor and offers insight for development of novel anti-HCV regimens.

Hepatitis C virus (HCV) belongs to a member of *Flaviviridae* and is a worldwide infectious pathogen causing chronic hepatitis that can progress further to hepatocellular carcinoma [1]. The current therapeutic protocol for HCV infection consists mainly of interferon (IFN) in combination with ribavirin that usually accompanies with strong side effects and moderate successful rate [2,3]. Hence, there is an urgent need to find new regimens to increase the efficacy of anti-HCV therapy.

Natural products metabolized from plants represent desirable sources for novel therapeutic compounds. Both *Lonicera hypoglauca* Miq. and *Lonicera japonica* Thunb are widely used as Jinyinhua in traditional Chinese medicine. Although they have similar geographic distribution, obviously various characteristics are observed [4]. Studies of the phytochemistry and bioactivity of Jinyinhua have mostly focused on *L. japonica* (Japanese honeysuckle) that has been reported to possess properties of anti-inflammation, anti-angiogenic, and anti-nociceptive activities [5,6]. However, the cognate *L. hypoglauca* has barely been studied.

Recently, the subgenomic HCV replicon cells have been developed for mechanistic study of HCV replication [7,8]. In the present study, HCV replicon cells were used to explore whether the extracts from *L. hypoglauca* elicit any anti-HCV activity. We found that *L. hypoglauca* contains an active phytocompound pheophytin a that exhibits strong anti-HCV activity. The inhibition of NS3 protease activity accounts mainly for the anti-HCV activity of pheophytin a. Furthermore, the combination of pheophytin a with INFα-2a elicits synergistic anti-HCV activity with no considerable cytotoxicity. The significance of these findings is discussed.

Materials and methods

Cell culture and viability assay. The subgenomic HCV replicon cells (a kind gift from Professor J.-H. James Ou, University of Southern California), the Huh7/Rep-Feo subgenomic replicon cells containing a luciferase reporter gene, and the Huh7.5 cells (a kind gift from Professor Charles Rice, The Rockefeller University, NY) were cultured as described [9–11]. Cell viability was determined

* Corresponding author. Fax: +886 04 22022073.
E-mail address: jccheng@mail.cmu.edu.tw (J.-C. Cheng).
[1] These authors contributed equally to this work and are considered as co-first authors.
[2] These authors contributed equally to this work.

0006-291X/$ - see front matter © 2009 Elsevier Inc. All rights reserved.
doi:10.1016/j.bbrc.2009.05.043

by trypan blue exclusion and MTS assay as described by the manufacturer (Promega).

Replicon cell-based assay (Western blot, luciferase, and RT-PCR assay). For HCV replicon cell-based bioactivity-guided screening, the extracts or compounds isolated from *L. hypoglauca* were ectopically applied to the replicon cells for 48 h. The expression of HCV viral proteins was determined by Western blot analysis as described previously [12]. On the other hand, the Huh7/Rep-Feo cells (2×10^5 cells) were seeded in a 6-well plate. At 8 h after seeding, the tested compound was added and incubated for a total of 120 h. The cells were then subjected to luciferase activity assay using the Bright-Glo luciferase assay system (Promega). The IC_{50} was defined as the concentration of compound at which the luciferase activity in the replicon cells was reduced by 50%.

For real-time RT-PCR analysis, total RNA was amplified using the forward primer HCV-F (5′-TGCGGAACCGGTGAGTACA-3′) and the reverse primer HCV-R (5′-CTTAAGGTTTAGGATTCGTGCTCAT-3′) in the presence of SYBR Green I Master Mix (Applied Biosystems). For internal control, RT-PCR was performed using the forward primer β-actin-F (5′-TCACCCACACTGTGCCCATCTACG-3′) and the reverse primer β-actin-R (5′-CAGCGGAACCGCTCATTGCCAATG-3′). The reaction condition was 1 cycle of 48 °C for 30 min., 1 cycle of 95 °C for 10 min, and 40 cycles of 95 °C for 15 s followed by 60 °C for 1 min.

Infectious HCV particles production and infection inhibition assay. The production of infectious HCV particles (HCVcc) was performed using the plasmid PFL-J6/JFH (a kind gift from Professor Charles Rice, The Rockefeller University) as described [13]. For infection inhibition assay, 100 μl of HCVcc-containing supernatant (5×10^3 foci forming units) was added to Huh7.5 cells and incubated for 4 h. The virus-containing supernatant was then removed and fresh medium with or without the tested compound was added and incubated for a total of 72 h. The cells were fixed and stained by anti-Core antibody (Affinity BioReagents) and the infectious foci were counted by the fluorescence microscopy.

Extraction. Leaves and stems of *L. hypoglauca* were collected from the Da-kang area of Taichung County in central Taiwan. The species were identified and voucher specimens (*YHT001* (TCF)) were deposited at the Herbarium of the Department of Forestry, National Chung Hsing University, Taiwan. The preparation and purification of crude extracts were performed as mentioned (Supplemental methods).

Molecular modeling of the pheophytin a-HCV NS3/4A complexes. The model of pheophytin a in complex with the HCV-NS3/4A protease was constructed by docking pheophytin a to the crystallographic structure of 1b strain of the HCV-NS3/4A protease (PDB code 1DY8) [14]. Molecular modeling was performed as mentioned (Supplemental methods).

NS3 serine protease activity assay. The NS3 serine protease activity assay was conducted by the FRET-based, SensoLyte™ HCV protease assay kit (AnaSpec). Briefly, HCV-NS3/4A protease was mixed with the tested compound in the assay buffer. After 15 min incubation at room temperature, 50 μl of FRET peptide substrate solution was added and mixed well. For kinetic reading, the fluorescence intensity was measured immediately and continuously at Ex/Em = 490 nm/520 nm. The data was recorded every 5 min for a total of 120 min.

Synergy analysis. To determine whether the effect for the combination of pheophytin a with INFα-2a (Roche) was synergistic, additive or antagonistic, the luciferase-based HCV replicon assay was performed and analyzed according to the classical isobologram analysis [15].

Statistical analysis. The Student's *t* test was used to evaluate the difference between the test sample and solvent control. $p < 0.05$ was considered statistically significant.

Results

Lonicera hypoglauca exhibits potent anti-viral activity in HCV replicon cells

In this study, HCV replicon cells were used to perform bioactivity-guided screening to explore whether the extracts from *L. hypoglauca* elicit any anti-HCV activity. The replicon cells were treated with various concentrations of EtOH-soluble extract (LH-crude) from *L. hypoglauca*. LH-crude caused a dose-dependent inhibition of NS5A expression, a long half-life HCV protein, without affecting cell viability and cell growth (Fig. 1A). Subsequent tracking of LH-crude revealed that the ethyl acetate-soluble fraction (LH-EA) but not the H_2O-soluble fraction (LH-water) was most active (Fig. 1B).

To identify the active component in LH-EA with anti-HCV activity, LH-EA was separated into 20 fractions (LH-EA-1 to -20) by

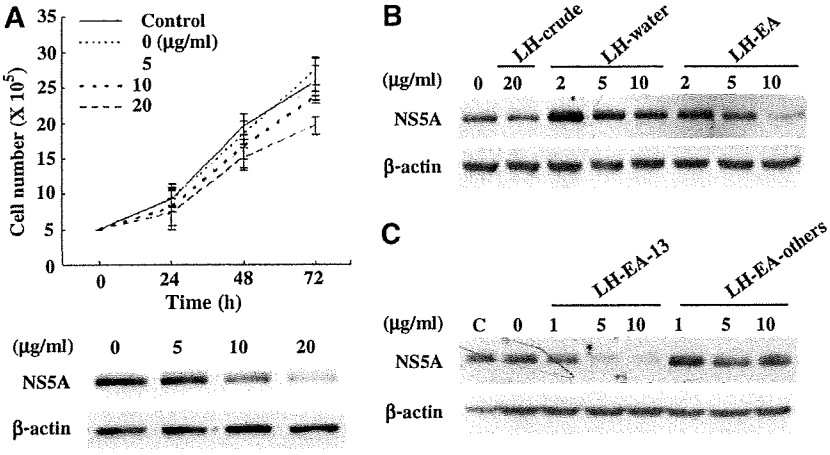

Fig. 1. *Lonicera hypoglauca* exhibits potent anti-viral activity in HCV replicon cells. (A) HCV replicon cells were treated with the indicated concentrations of EtOH extract (LH-crude) from *L. hypoglauca* and viable cells were determined by the trypan blue exclusion analysis. The data represented the means ± SD. ($n = 3$, upper panel). The cell lysates (48 h post-treatment) were subjected to Western blot analysis using the anti-NS5A antibody (lower panel). (B, C) HCV replicon cells were treated with the indicated concentrations of LH-crude, EtOAc-soluble fraction (LH-EA), H_2O-soluble fraction (LH-water), the fraction 13 of LH-EA (LH-EA-13), and the pool of other LH-EA fractions (LH-EA-others), respectively. The cell lysates (48 h post-treatment) were subjected to Western blot analysis using the anti-NS5A antibody. The expression of β-actin was used for the control of equal protein loading. C:No-treated, control replicon cells.

chromatography. Each fraction was further evaluated for their anti-HCV activity using the same replicon cell-based assay. As shown in Fig. 1C, the fraction of LH-EA-13 exhibited the strongest anti-HCV activity.

Pheophytin a reduces HCV protein expression in replicon cells and the infectivity of HCVcc

To understand which compound exhibits anti-HCV activity, the LH-EA-13 fraction was purified by HPLC to obtain compound 1. The compound 1 molecular formula was determined to be $C_{55}H_{74}N_4O_6$ (MW = 887.23) by fast atom bombardment mass spectrometry. The ^{1}H NMR spectrum of compound 1 presented 1.68 (t, J = 8 Hz, 3H), 1.79 (d, J = 7.2 Hz, 3H), 2.16 (m, 1H), 2.31 (m, 1H), 2.45 (m, 1H), 2.59 (m, 1H), 3.23 (s, 3H), 3.39 (s, 3H), 3.67 (s, 3H), 3.68 (q, J = 8 Hz, 2H), 3.85 (s, 3H), 4.19 (d, J = 9.2 Hz, 1H), 4.50 (dq, J = 7.2, 5.2 Hz, 1H), 6.17 (dd, J = 11.6, 1.6 Hz, 2H), 6.24 (s, 1H), 6.28 (dd, J = 18.0, 1.6 Hz, 2H), 7.99 (dd, J = 18.0, 11.6 Hz, 1H), 8.54 (s, 1H), 9.38 (s, 1H), and 9.51 (s, 1H). The ^{1}H NMR spectrum of compound 1 was identical to the spectrum of pheophytin a which has been identified by Ina and his coworker [16]. The structure of pheophytin a was shown in Fig. 2A. The purity of pheophytin a was estimated to be greater than 99.5% from the ^{1}H NMR spectrum and HPLC analysis.

We then used compound 1 (pheophytin a) to confirm its anti-HCV activity using HCV replicon cells and Huh7/Rep-Feo cells. Pheophytin a did not affect the cell viability of these cells (Fig. 2B left panel, Fig. 2C upper panel). However, it was more potent than the crude extracts in inhibiting NS5A expression in replicon cells (Fig. 2B right panel) and luciferase expression in Huh7/Rep-Feo cells (Fig. 2C lower panel). Pheophytin a also significantly inhibited replicon cells HCV RNA accumulation (Fig. 2D) and the infectivity of HCVcc (Fig. 2E, $p < 0.05$). The calculated IC_{50} was 4.97 μM. These data thereby unveil pheophytin a as the active component of *L. hypoglauca* with anti-HCV activity.

Computational molecular modeling reveals the interaction of pheophytin a with the active site of HCV-NS3 protease

NS3 protease is an attractive target for development of antiviral agent. To gain more chemical insight for the molecular mechanism involved in the anti-HCV activity of pheophytin a, computational molecular modeling was performed by docking pheophytin a onto the active site of HCV NS3/4A. The best predicted binding mode was illustrated in Fig. 3A and B. The amino acids HIS57, LYS136, SER139, and ALA155 were involved in the formation of four hydrogen bonding with pheophytin a. In addition, the amino acids SER42, GLY137, LYS136, VAL132, SER133, CYS159, PHE154,

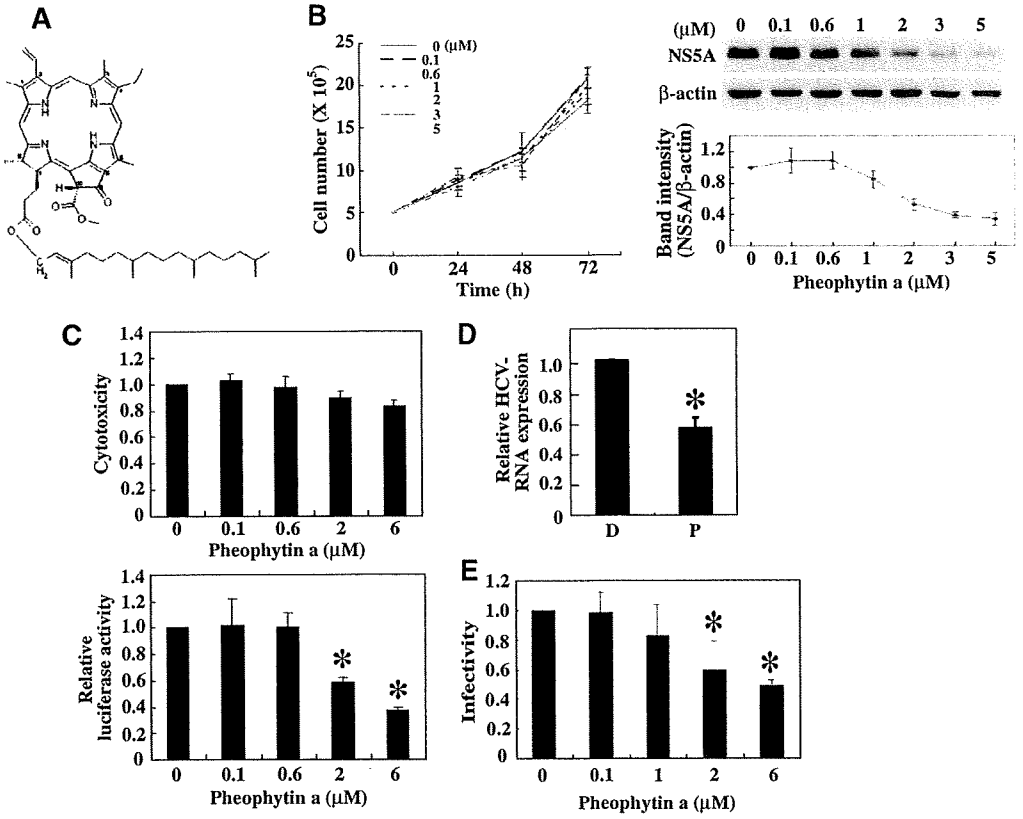

Fig. 2. Pheophytin a inhibits HCV expression in the subgenomic HCV replicon cells and HCVcc. (A) Chemical structure of pheophytin a. (B) HCV replicon cells were treated with the indicated concentrations of pheophytin a and the viable cells were determined by the trypan blue exclusion analysis (left panel). The cell lysates (48 h post-treatment) were subjected to Western blot analysis using the anti-NS5A antibody and the expression of β-actin was used for the control of equal protein loading (right panel). The band intensity of NS5A versus β-actin was determined and the ratios were plotted against the concentration of pheophytin a. (C) Huh7/Rep-Feo cells were treated with the indicated concentrations of pheophytin a. The cell toxicity was determined by MTS assay (upper panel) and the HCV gene expression was determined by luciferase activity assay (lower panel). (D) HCV replicon cells were treated with 6 μM of pheophytin a for 96 h and the total RNA was subjected to real-time RT-PCR assay. The relative HCV-RNA level for pheophytin a- (P) and DMSO-treated (D) control cells was shown. (E) The HCVcc-infected Huh7.5 cells were treated with various concentration of pheophytin a. The cells were stained by the anti-Core antibody and the relative infectivity for the indicated treatment compared to the control treatment cells was shown. *$p < 0.05$ when compared to the control replicon cells. The data represented the mean ± SD (n = 3).

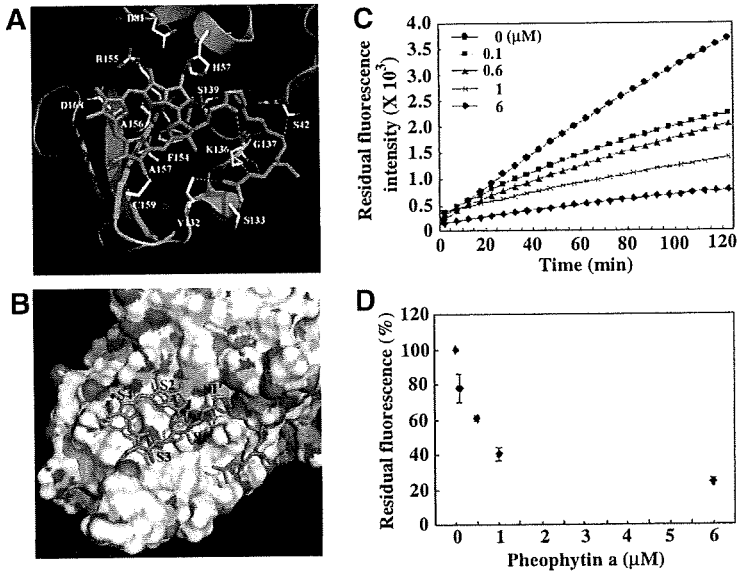

Fig. 3. Computational molecular models and molecular analysis for the interaction between pheophytin a and HCV NS3/4A. (A, B) The computational molecular models of pheophytin a in the active site of the HCV NS3/4A were shown as cartoon and surface in (A) and (B), respectively. The carbon atoms in pheophytin a were colored in magenta. The side-chains of the NS3 amino acid residues within 5 Å radius centered on pheophytin a were shown explicitly. The carbon atoms in NS3 were shown in gray. Nitrogen and oxygen were colored in blue and red, respectively. Trace of the NS3 backbone structure was shown as a blue tube. The secondary structure elements were shown as a ribbon drawing and the important amino acid residues involved in pheophytin a binding were labeled. The green and yellow dotted lines represented tentative donor–acceptor pairs of the hydrogen bonds and the hydrophobic interactions between pheophytin a and NS3, respectively. (C, D) HCV-NS3/4A protease (5 ng/well) was mixed with the indicated concentrations of pheophytin a and the *in vitro* protease activity was determined as described in "Materials and methods". The fluorescence signal was recorded every 5 min (C). The percentage of residual activity at 60 min after initiation of reaction was calculated and was plotted against the concentration of pheophytin a (D). The data represented the means ± SD ($n = 3$).

ALA156, ASP168, and ARG155 also contributed to the hydrophobic interactions and binding with pheophytin a. An important noncovalent hydrogen bond interaction was formed between the hydroxyl group of SER139 of the NS3 catalytic triad and the acyl oxygen in the ester group of pheophytin a. Furthermore, the S1, S2, S3, and S4 sites of NS3 were probably occupied by the porphin group of pheophytin a, and the S′ sites other than S1′ were possibly occupied by a phytol group of pheothytin a. The particular hydrophobic interaction was formed between a phytol group of pheophytin a and a long nonpolar chain of four carbon atoms of LYS136. These data suggest that pheophytin a may have a functional interplay with HCV-NS3.

Pheophytin a elicits its anti-HCV effect by inhibition of NS3 serine protease activity

To further delineate the effect of pheophytin a on HCV-NS3, the NS3 serine protease activity assay was performed in the presence of pheophytin a. The amount of fluorescence signal was decreased with increasing concentration of pheophytin a in a dose-dependent manner (IC_{50} = 0.89 μM), indicating that pheophytin a exhibits the anti-NS3 serine protease activity (Fig. 3C). Plotting the residual protease activity of reactions containing various concentrations of pheophytin a as percentage of activity in the absence of the compound (expressed as 100%) resulted in a titration curve typical of a binding inhibitor (Fig. 3D).

Combination of pheophytin a with INFα-2a significantly enhances anti-HCV activity without an increase in cytotoxicity

To determine whether pheophytin a and INFα-2a have synergistic inhibitory effect on HCV gene expression, the classic isobologram analysis was performed. A typical isobologram used to measure the drug–drug interaction was shown in Fig. 4A with synergy, additivity, and antagonism presented as concave, linear and convex isoeffective curves, respectively [17]. Our results demonstrated that the curve was below the line representing additive effect, indicating the synergy of the two drugs against the replicon cells (Fig. 4B). In addition, MTS assays did not show any difference in cell survival with the drug concentrations used in this isobologram analysis (data not shown), suggesting that the synergistic effect of pheophytin a and INFα-2a on HCV gene expression is not due to cytotoxicity.

Discussion

The global prevalence of HCV infection averages 3% according to the estimation made by the World Health Organization. Through bioactivity-guided screening, structure–activity relationship, and biochemical analysis, we report herein that HCV-NS3 is a potent molecular target of *L. hypoglauca*-derived pheophytin a. As a result, the viral proteins and RNA expression and the HCV infectivity are diminished. Notably, concomitant treatment of HCV replicon cells with pheophytin a and INFα-2a elicits synergistic effect and enhances anti-HCV activity without compensation of cell survival. This study thereby offers insight to the molecular basis for the anti-HCV activity of *L. hypoglauca* and indicates pheophytin a as a potent adjuvant regimen for INFα-2a therapy in the clinical setting.

Among the HCV nonstructural proteins, NS3-mediated processing of the protein junctions is essential for viral replication and therefore provides an attractive target for development of antiviral agents [18]. In addition to pheophytin a, several studies also discovered natural products with anti-NS3 protease activity. These include nature compounds from Galla Chinese and *Rhodiola kirilowii*